



THE EFFECT OF A MAGNETIC FIELD ON THE THERMOPOWER OF SILVER-GOLD ALLOYS

Ву

Michael J. O'Callaghan

A THESIS

Submitted to
Michigan State University
in partial fulfillment of the requirements
for the degree of

MASTER OF SCIENCE

Department of Physics

ABSTRACT

THE EFFECT OF A MAGNETIC FIELD ON THE THERMOPOWER OF SILVER-GOLD ALLOYS

Ву

Michael J. O'Callaghan

Four dilute alloys of silver-gold were prepared in the form of long polycrystalline wires. The change in thermoelectric voltage was measured due to the presence of tranverse magnetic fields up to 50 kG. Measurements were made from 4.2°K up to 48°K. From this data the change in thermopower ΔS was obtained by fitting the voltage vs. temperature data to a curve and differentiating.

It was found that the magnetic field enhanced the thermopower and that a peak occurs in ΔS at about the same temperature as the peak in the zero field thermopower. The position of the peak in ΔS shows very little dependence on magnetic field strength. It does, however, move to higher temperatures with increasing gold concentration. The behavior of ΔS does not correlate well with the quantity $\omega \tau$, where τ is the relaxation time for an electron in the alloy and ω is the cyclotron frequency of a free electron.

ACKNOWLEDGEMENTS

I wish to thank Dr. Peter A. Schroeder for suggesting the problem and for his assistance and guidance in conducting this work.

Financial support by the National Science Foundation is gratefully acknowledged.

TABLE OF CONTENTS

Chapter		Page
I	INTRODUCTION	1
II	THEORY	2
	Diffusion Thermopower Phonon Drag Thermopower Magnetic Field Effects Impurities	5 7 10 13
III	EXPERIMENTAL APPARATUS	15
	Cryostat	16
IV	SAMPLE PREPARATION	25
V	DATA ANALYSIS	27
VI	DISCUSSION OF RESULTS	31
Appendix		
A	Calibration Data for Resistance Thermometer	47
В	Computer Program Used to Fit EMF Data to a Polynomial	48
References		55

LIST OF TABLES

Table		Page
1	Data on Ag-Au Alloys	32
2	Calibration Data for Resistance Thermometer	47
3	Coefficients used for Polynomial fit to Resistance Data	48

LIST OF FIGURES

Figure		Page
1	Thermocouple schematic	4
2	Thermoelectric currents	6
3	Electron-phonon scattering processes	9
4	The Fermi surface of silver ⁸	11
5	Method for directly measuring the change in thermopower	17
6	Schematic of cryostat sample mount	18
7	Cryostat-solenoid geometery	19
8	Electronics	21
9	Thermometer resistance	28
10	EMF vs. T	30
11	Effect of oxygen anneal	34
12	Resistivity vs. T	35
13	Variation of ΔS with concentration (50 kG)	36
14	ΔS vs. H	38
15	Zero field thermopower ⁷	39
16	$\Delta S/T$ vs. T^2	41
17	TΔS vs. T ²	42
18	Change in S of Ag + .011 at. % Au	43
19	Change in S of Ag + .013 at. % Au	44
20	Change in S of Ag + .047 at. % Au	45
21	Change in S of Ag + .048 at. % Au	46

CHAPTER I

INTRODUCTION

In previous studies of the effects of a magnetic field on the thermopower of a conductor it has been unclear what contribution to the total thermopower was being changed. Theoretical consideration of diffusion thermopower¹ and phonon drag thermopower² are both compatible with experimentally observed magnetic field dependences. Observing the magnetic field effects on dilute alloys may be of some use in deciding between the two models.

Dilute silver-gold alloys have been chosen for the following reasons.

- (1) They are readily soluble in one another.
- (2) Extensive measurements have been made of their transport properties.
- (3) Since the gold is much heavier than silver it is a good scatterer of phonons. Since gold is homovalent with silver, it is a comparatively poor scatterer of electrons. These properties will be useful in differentiating between phonon drag and diffusion effects.

The purpose of this thesis is to describe the experimental apparatus and methods used to study the effects of magnetic fields on the thermopower of dilute alloys and then to discuss the results of those measurements.

CHAPTER II

THEORY

When a temperature gradient is maintained in a conductor an associated electrical potential gradient is also created. The ratio of the electric field -dV/dx to the temperature gradient dT/dx at a particular temperature defines the thermopower S at that temperature.

$$S = -\frac{dV/dx}{dT/dx} = -dV/dT$$
 (2.1)

The potential difference between the two ends of the conductor can then be written as:

EMF =
$$-\int_{x_1}^{x_2} dV/dx dx = \int_{x_1}^{x_2} S dT/dx dx = \int_{T_1}^{T_2} S dT$$
 (2.2)

Where T_1 and T_2 are the temperatures at the ends of the conductor. This expression has the advantage that it depends only on the temperatures at the ends of the conductor and on the variation of S with temperature. It does not depend on the details of the temperature gradient.

In order to measure the EMF across a conductor leads must be used to make a connection to a voltage measuring device. These leads have a thermopower of their own and will be subjected to temperature

differences which will cause them to generate their own thermoelectric voltage which will be in addition to the EMF that is to be measured. This situation is depicted in Figure 1. If the conductor has thermopower $S_{\mbox{A}}$ and the leads have thermopower $S_{\mbox{L}}$ then the EMF actually measured will be:

$$EMF = \int_{T}^{T_{1}} S_{L} dT + \int_{T_{1}}^{T_{2}} S_{A} dT + \int_{T_{2}}^{T} S_{L} dT = \int_{T_{1}}^{T_{2}} (S_{A} - S_{L}) dT = \int_{T_{1}}^{T_{2}} S_{AL} dT$$
 (2.3)

where \mathbf{S}_{AL} is the effective thermopower of the conductor-lead combination. The EMF measured is actually the difference in the EMFs generated by the two conductors. This is referred to as the Seebeck effect.

Since the EMF depends only on T_1 and T_2 the Seebeck effect is useful for measuring temperature differences electrically. This is the principle of operation for thermocouples.

The thermopower of a conductor is commonly broken up into two components, the diffusion thermopower $\mathbf{S}_{\mathbf{d}}$ and the phonon drag thermopower $\mathbf{S}_{\mathbf{q}}$. The total thermopower is just the sum of the two:

$$S = S_d + S_q \tag{2.4}$$

Some theoretical work has been done 3 suggesting that there may be an interference term between S_d and S_g but that it is small enough that the two components may be added linearly to a high degree of accuracy.

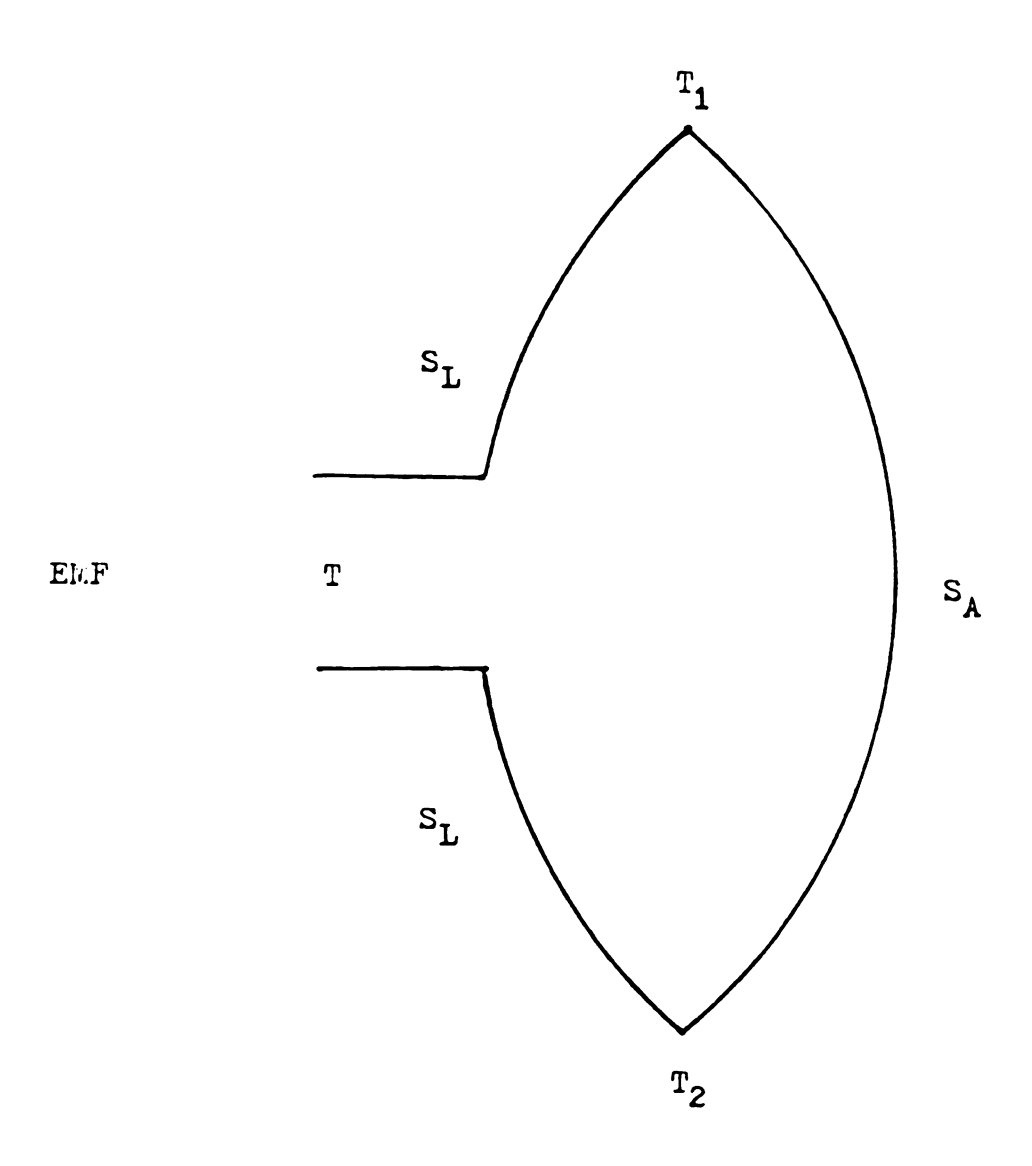


Fig. 1 Thermocouple schematic

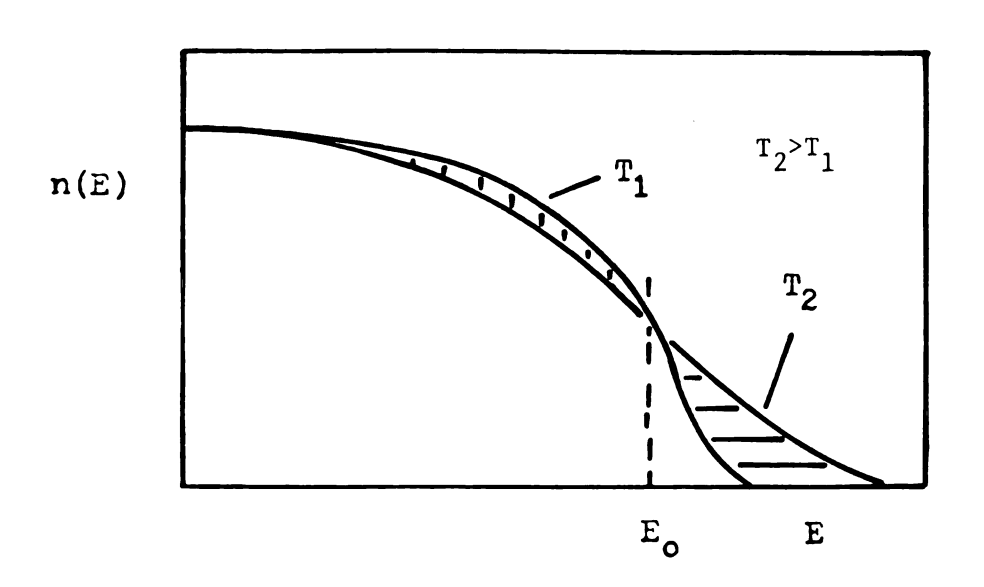
Diffusion Thermopower

The diffusion thermopower is derived by considering the electrons to be interacting with phonons and randomly distributed scattering centers at local thermal equilibrium. The electrons are considered to have an energy dependent relaxation time and consequently an energy dependent electrical conductivity. The expression for S_d can be shown to be: 4

$$S_{d} = \frac{\pi^{2} k^{2} T}{3e} \left(\frac{\partial \ln \sigma}{\partial E} \right)_{E_{f}}$$
 (2.5)

where k is Boltzmann's constant, E the electron energy, σ the electrical conductivity, e the electron charge, and E_f is the Fermi energy. This expression is valid for $T>\theta_D$ (Debye temperature) or at low temperatures when impurity scattering is dominant; in both cases S_d is proportional to T.

The importance of the energy dependent electrical conductivity can be illustrated with the situation depicted in Figure 2. The electron energy distributions should look somewhat as shown in the graph for the two temperature regions. Clearly the electrons above E_0 will diffuse towards the low temperature region and the electrons below E_0 will diffuse to the higher temperature region. If $\sigma(E)$ is sufficiently small for $E > E_0$ then the net current will be towards the low temperature region and the cold end will become electrically positive, resulting in a negative thermopower. On the other hand, if $\sigma(E)$ is small for $E < E_0$ then the net current would be towards the hot end, resulting in a negative thermopower. The diffusion thermopower can be either positive or negative depending on the energy dependence



current towards cold end
current towards hot end

Fig. 2 Thermoelectric currents

of the electrical conductivity, or equivalently it depends on the variation of the relaxation time with energy. One other characteristic that will be shown to be of importance in a magnetic field is the variation of the relaxation time over the Fermi surface for a given energy.

Phonon Drag Thermopower

Phonon drag thermopower arises from the following mechanism. As phonons carry heat from one end of a conductor to the other they can interact with electrons. In these interactions momentum is exchanged and the electron flow will be influenced. Since the electrons may gain a net momentum, the phonon interactions could lead to the electrons being piled up at one end of the conductor. This redistribution of electrons would produce an electrical potential difference between the hot and cold ends of the conductor.

There are two basic types of electron-phonon interactions, the so called normal and umklapp processes. In the normal process the phonon and electron momenta are related by:

$$\vec{K}' - \vec{K} \pm \vec{q} = 0 \tag{2.6}$$

where \vec{q} is the phonon momentum and \vec{k} , \vec{k}' are the initial and final momenta of the electron. In this type of process for a spherical Fermi surface the phonons impart momentum to the electrons in the direction of the phonon flux. This represents a negative contribution to the thermopower.

In the umklapp process the momenta are related by:

$$\vec{K}' - \vec{K} \pm \vec{q} = \vec{g}$$
 (2.7)

where \vec{g} is a reciprocal lattice vector. For a spherical Fermi surface an electron would gain momentum in the direction opposite to that of the phonon flux. Both processes are illustrated in Figure 3. The umklapp process can contribute a positive component to the thermopower.

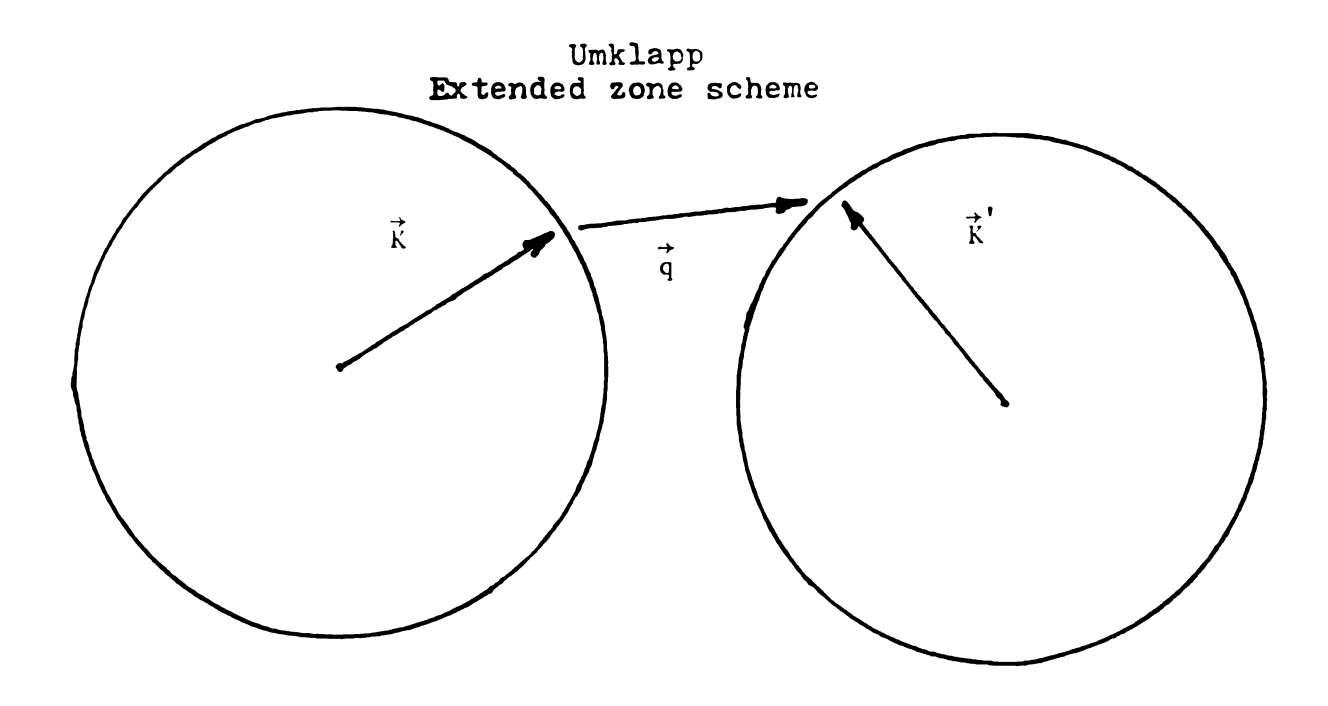
The situation is more complex for non-spherical Fermi surfaces, but the main point is that contributions to $\mathbf{S}_{\mathbf{g}}$ of either sign are possible. Which of the scattering processes becomes dominant depends on the detailed nature of the Fermi surface.

The temperature dependence of the phonon drag thermopower can be estimated as follows. S_{α} may be written:

$$S_g = \frac{C_g}{3Ne} \frac{\tau_{pp}}{\tau_{pp}^{+\tau_{pe}}}$$
 (2.8)

where C_g is the lattice specific heat, N is the electron density, e the electronic charge, τ_{pp} is the phonon-phonon relaxation time and τ_{pe} is the relaxation time for phonon-electron interactions. At low temperatures p-e interactions dominate and so $\tau_{pe}^{<\tau_{pp}}$. Since C_g is proportional to T^3 at low temperatures we have that S_g is proportional to T^3 over this same temperature range. At relatively high temperatures $\tau_{pp}^{<\tau_{pe}}$ and C_g remains nearly constant. It can be shown that τ_{pp} is proportional to T^{-1} for the higher temperatures, and so S_g is proportional to T^{-1} in this temperature range.

The total thermopower may now be written as $S = AT + BT^3$ in the low temperature range and as $S = AT + BT^{-1}$ in the high temperature range.



Normal Reduced zone scheme

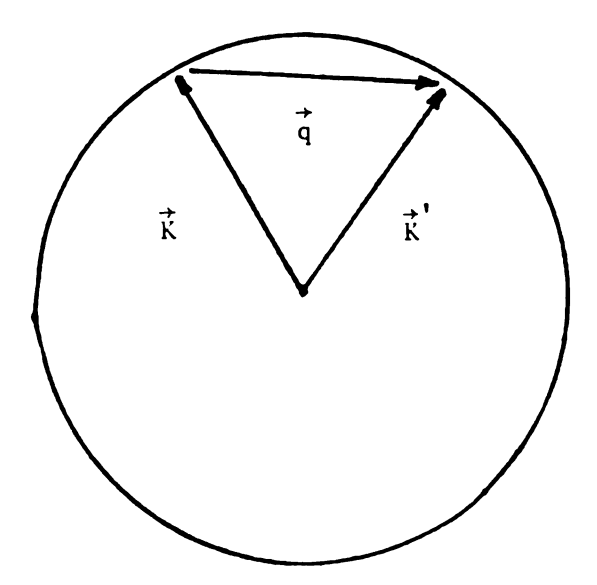


Fig. 3 Electron-phonon scattering processes

Magnetic Field Effects

When a magnetic field is applied to a conductor, essentially the only thing affected is the motion of the electrons. The phonon spectrum, the Fermi surface, and the electron energy levels are not affected in any relevant way. The consequence of this is that the mechanisms thought responsible for thermoelectric phenomena are left unaffected; the only direct effect is on the motion of the electrons. A drawing of the Fermi surface of silver is shown in Figure 4. The phonon drag effect is predominantly of the umklapp variety for electrons in the portions of the surface intersecting the Brillouin zone boundaries (the neck regions) and primarily of the normal type of phonon scattering event in the other regions (the belly regions). Typically both the velocity and relaxation time for electrons in the neck regions are smaller than in the belly regions, consequently electrons in the neck regions are closer to being in thermal equilibrium than those in the belly regions.

When a magnetic field is applied, the electrons begin to follow cyclotron orbits around the Fermi surface; some of these orbits traverse the neck regions. As these electrons pass from the neck region (where they have had a near equilibrium energy distribution) to the belly region, their original distribution will not be affected too drastically due to the longer relaxation times in the belly region. Likewise, electrons traveling from the belly to the neck region will affect the energy distribution of electrons in the neck region. They will, however, be quickly redistributed in energy due to the short relaxation time. The energy distribution of electrons that move along purely belly orbits will be largely unaffected.

The net effect of the magnetic field, then, is to cause a redistribution of electrons both in energy and in location on the Fermi surface.

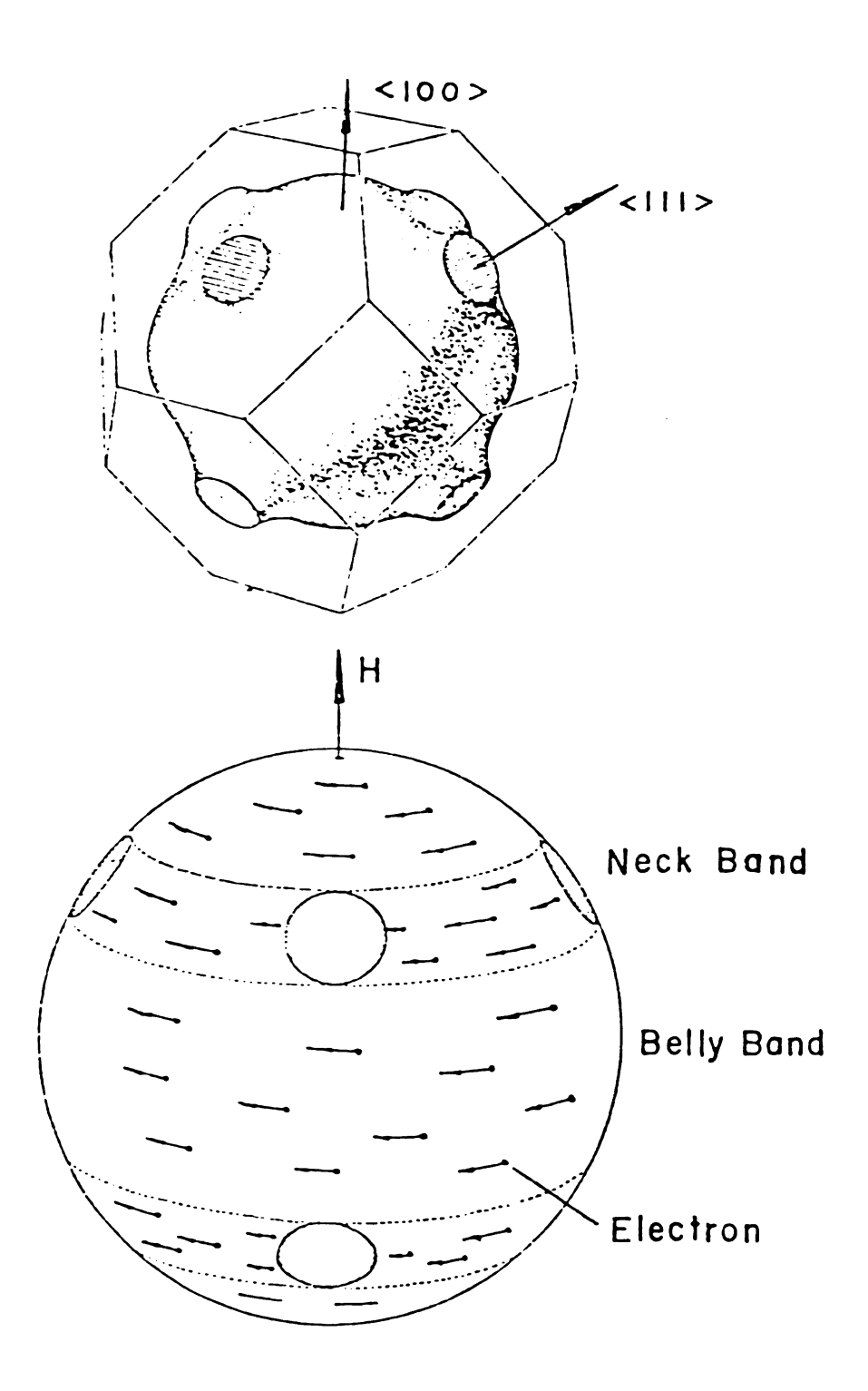


Fig. 4 The Fermi surface of silver ⁸

It might be expected that the number of electrons present in the neck regions would increase. Since the neck regions are sites of umklapp scattering, such a redistribution would lead to an enhanced positive thermopower.

The diffusion thermopower should also be affected since it depends critically on how many electrons are experiencing what relaxation time. For a given energy electrons can have any of a variety of relaxation times depending on whether they are in the neck or the belly regions. They might be described as having a relaxation time that is a weighted average of the relaxation times in the various regions. The redistribution caused by a magnetic field will clearly have an effect on this weighted average and will consequently affect the diffusion thermopower.

As the magnetic field increases, the effect it has should also increase. It is useful to consider the quantity $\omega\tau$ in this context; ω is the cyclotron frequency of the electron and τ its relaxation time. If $\omega\tau$ <<1 then an electron would barely start its cyclotron orbit before suffering a collision, and the effect of the field should be minimal. When $\omega\tau$ >>1 the field should reach peak effectiveness as the electrons are able to make several circuits of their cyclotron orbits before suffering a collision, and the effect of the field would reach saturation. Since τ decreases with increasing temperature, more intense magnetic fields should be required to reach saturation at higher temperatures.

Magneto-resistance reaches a saturation value in compensated materials but does not saturate for uncompensated materials. Thermo-power is expected to differ in that it should saturate for both compensated and uncompensated materials.

One approach that seems useful for understanding the effect of a magnetic field is the band model. In this model the thermopower is written as the sum of the individual thermopowers from differing portions of the Fermi surface:

$$S = \sum_{i} \frac{\sigma_{i}}{\sigma_{T}} S_{i}$$
 (2.9)

where σ_i is the electrical conductivity of the ith band, S_i is its thermopower, and σ_T is the total electrical conductivity. In the case of silver the relevant bands would be cyclotron orbits lying entirely in the belly regions and those orbits traversing the neck regions.

It has been shown for a two band uncompensated metal 1 that the band model predicts that S will reach a saturation value as $\omega\tau$ becomes much greater than one.

Impurities

Impurities in a conductor can have a significant effect on the thermopower. The simplest situation is when the electronic structure of the host and impurity atoms are the same. Electrons would not be greatly scattered by such impurities. The major effect would be the scattering of phonons due to the difference in mass between the host and impurity atoms. The phonon drag thermopower should be strongly affected.

If atoms with a different valence or with strong magnetic properties were introduced then electron scattering could be greatly altered. The electron diffusion thermopower could be greatly influenced in this case.

Silver and gold have the same outer electron configuration and so have similar electrical properties. For small concentrations of gold in silver the primary effect should be on the phonon drag thermopower. By studying the change of S in a magnetic field for various concentrations of gold in silver, it may be possible to tell how much of the change is due to phonon drag enhancement and how much to electron diffusion thermopower enhancement.

CHAPTER III

EXPERIMENTAL APPARATUS

There are two commonly used approaches to measuring the thermopower of a material. They are based on the equivalent relationships:

$$EMF = \int_{T_1}^{T_2} SdT \qquad S = -dV/dT \qquad (3.1)$$

These approaches are referred to as the integral method and the differential method.

In the differential method the differential form of the thermopower relationship is used. If the temperature difference across a sample is sufficiently small the thermopower can be obtained simply from the ratio of the voltage across the sample to the temperature difference. By raising or lowering the temperature of the entire sample the thermopower at various temperatures can be found. The experimental apparatus for these measurements is relatively cumbersome but the data analysis is quite simple.

The integral method uses the integral form of the thermopower relationship. If one end of the sample is maintained at temperature T_1 and V is recorded for various values of T_2 , the thermopower is given by $S(T_2) = -dV/dT_2$. One difficulty with this method is that for large temperature gradients there may be undesirable heat flow

through the sample. This problem may be minimized by using samples in the form of long thin wires.

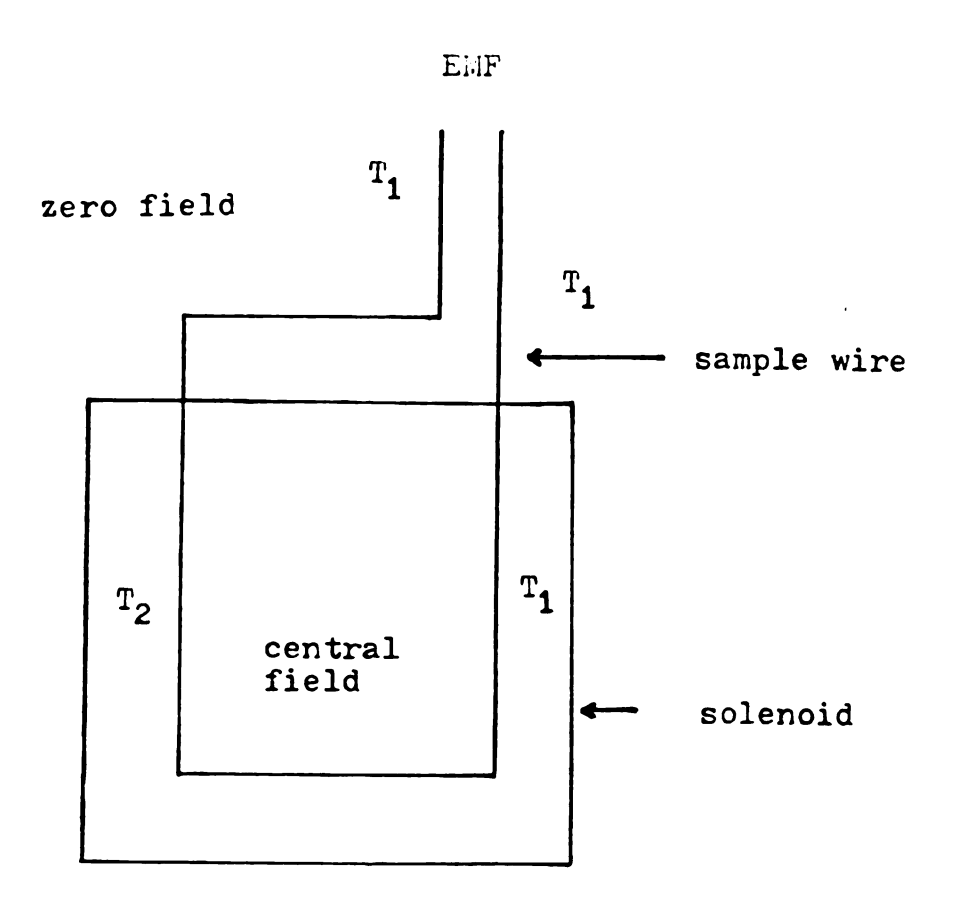
Another difficulty with the integral method is in the data analysis. The discrete data points for V vs. T must be fitted to a curve in order to find dV/dT. The differentiation can be carried out either graphically or numerically. The primary advantage of the integral method is its experimental simplicity.

For the measurements presented in this thesis a modification of the integral method due to Chiang⁶ is used. Since the thermopower of silver-gold alloys is fairly well established,⁷ the quantity of interest is the change of thermopower in the presence of a transverse magnetic field. This can be found directly with the arrangement shown in Figure 5. Since the sample is in the form of a long wire it will necessarily be polycrystalline. The measured thermopowers will be an angular average of the thermopower tensor.

Cryostat

A functional diagram of the cryostat used (constructed by R. Cady) is shown in Figure 6. In order to minimize heat conduction to the sample, the can containing it is evacuated typically to 10⁻² microns. For the same reason the base supporting the two rods is made of brass. The two rods which support the sample are made of copper in order to minimize any temperature gradients along them.

One of the hollow copper support rods is open to the surrounding liquid helium bath, which serves as the constant temperature region for the integral method of measuring the thermopower. The other hollow support rod serves as the variable temperature region. The top of the variable rod is connected to a small can that can be filled



$$EMF = \int_{T_1}^{T_2} S(H,T)dT + \int_{T_2}^{T_1} S(0,T)dT = \int_{T_1}^{T_2} \{S(H,T) - S(H,0)\}dT$$

$$\Delta S = \frac{dEMF}{dT_2} = S(H,T_2) - S(0,T_2)$$

Fig. 5 We thod for directly measuring the change in thermopower

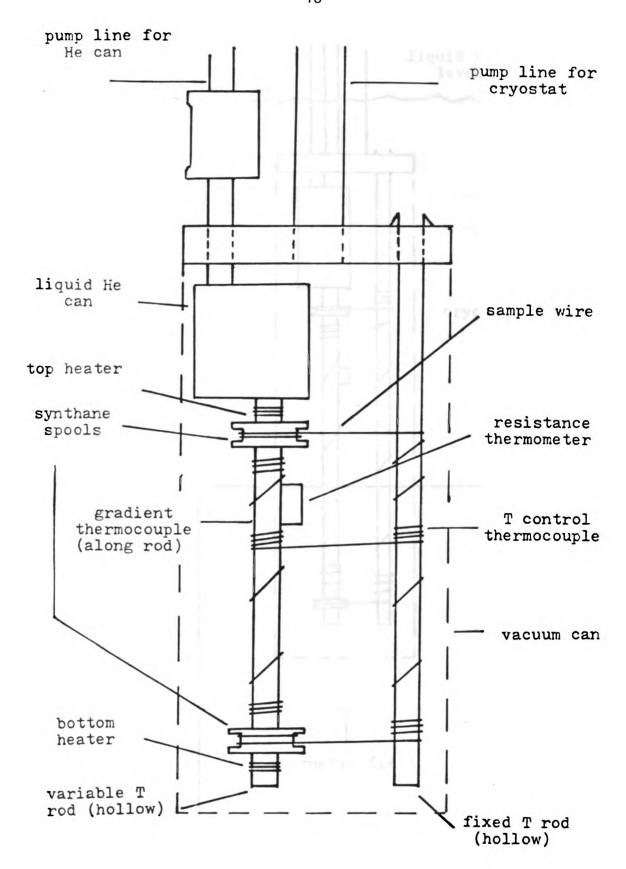


Fig. 6 Schematic of cryostat sample mount

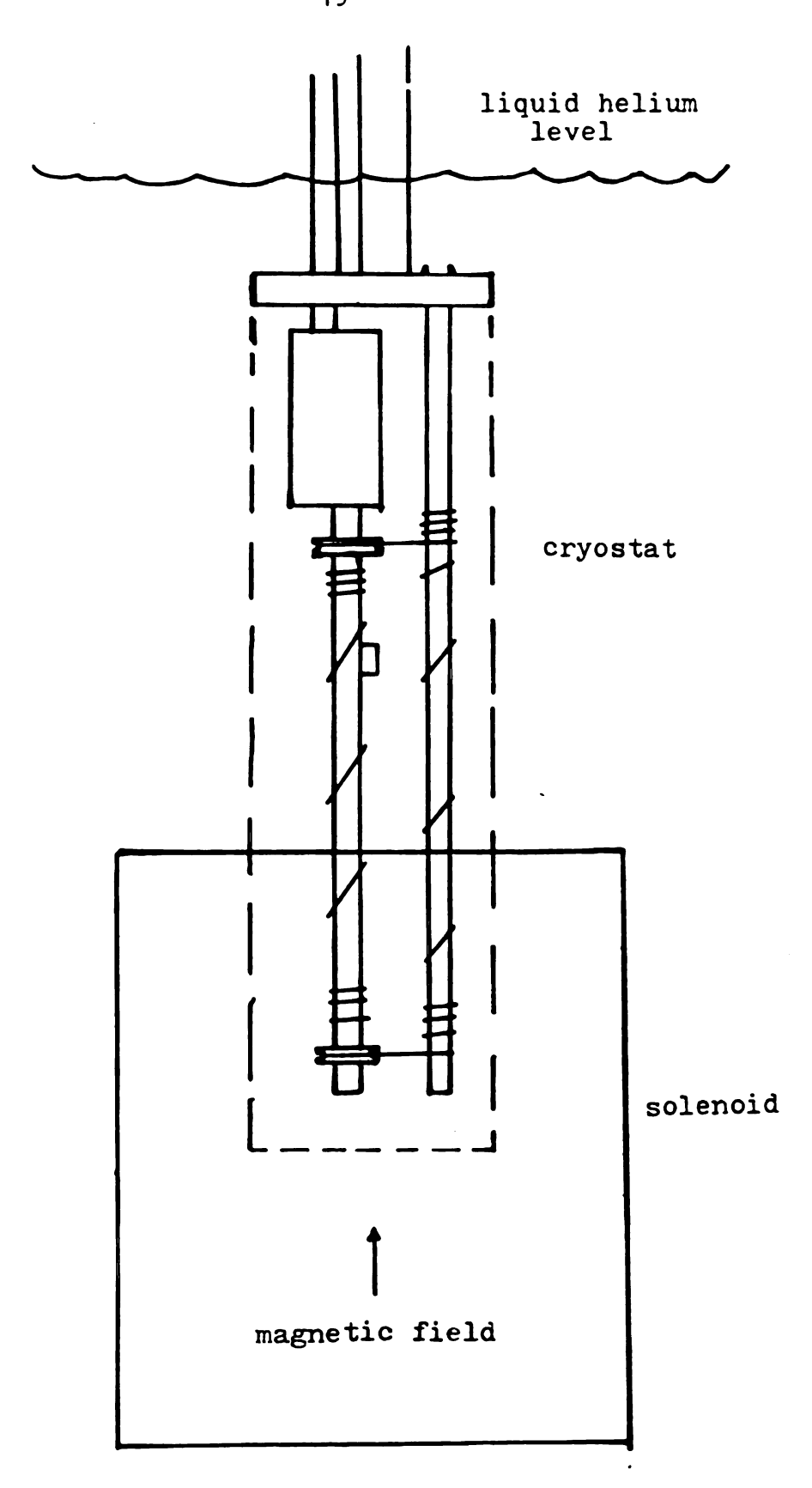


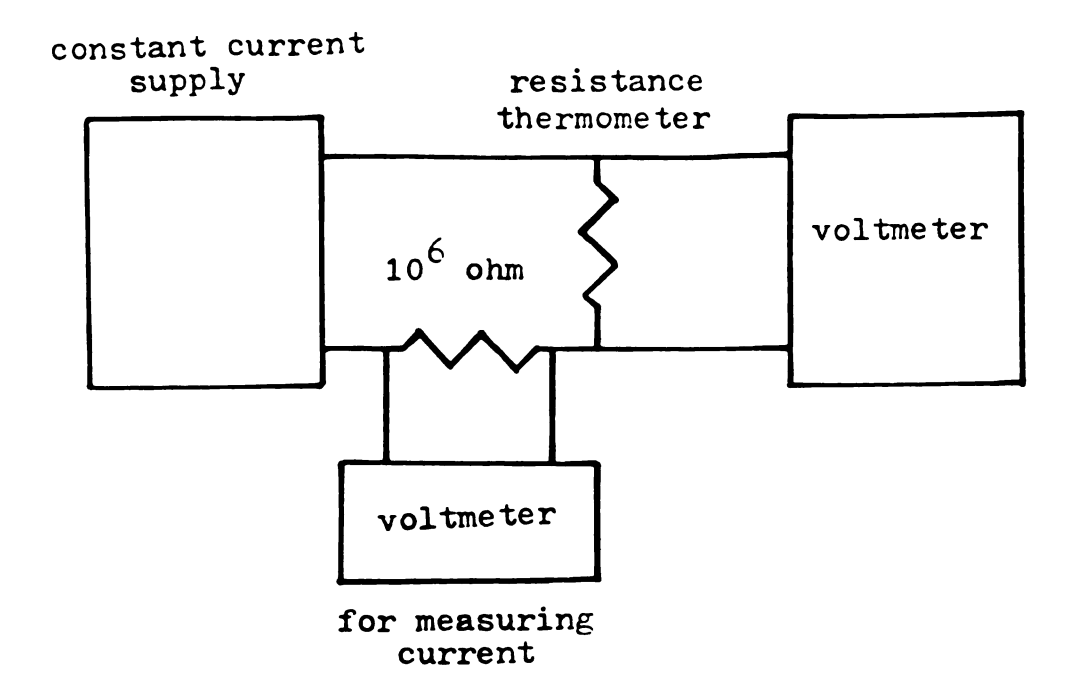
Fig. 7 Cryostat-solenoid geometery

with liquid helium from the surrounding bath. The temperature of this support rod can then be lowered below that of the surrounding helium bath by maintaining the helium in the can at reduced pressure. This cooling capability was not used for the purposes of this thesis; instead the temperature of the variable rod was raised to various levels between 4.2°K and 50°K. This was accomplished by the use of two electrical heating wires made of Evenohm wire which are positioned at the top and bottom of the rod as shown in Figure 6. The two heaters are used independently.

The only temperature that need be measured is that of the variable temperature rod. A difficulty is encountered here in that most types of temperature measuring devices are strongly affected by the presence of a magnetic field. To avoid this problem a carbon-glass resistance thermometer produced by Lake Shore Cryotronics, Inc. was used. It is expected that temperature measurement errors never exceeded one percent for the range of magnetic fields used. A diagram of the resistor circuit and for other circuitry is shown in Figure 8.

In order to simplify data taking the temperature is controlled electronically. A circuit controls current to the top heater so as to keep the voltage from a thermocouple, mounted between the two supports, constant. This constant is determined by an adjustable voltage reference. By using this control scheme it is very easy to adjust the temperature in small increments simply by changing the value of the reference voltage. The fact that the thermopower of the thermocouple is affected by the presence of a magnetic field is of no importance in this application.

A second thermocouple mounted along the length of the variable temperature rod detects any thermal gradient that may exist along



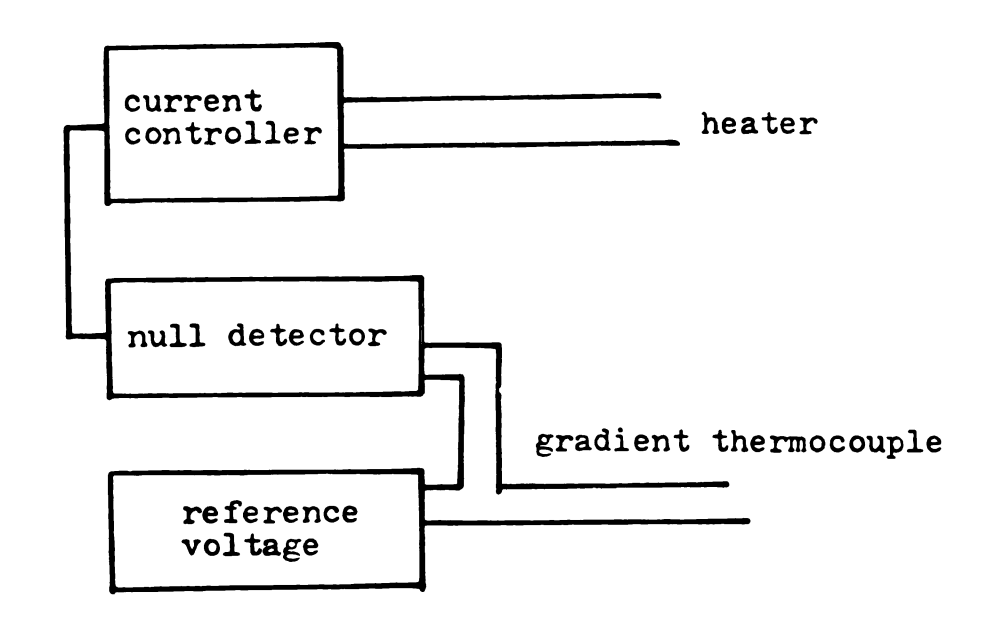


Fig. 8 Electronics

this rod. The gradient is reduced to negligible proportions by adjusting the current to the bottom heater. By using this method the temperature was kept uniform to within a third of a degree.

If care is not taken in the physical placement of the wiring, temperature gradients may be created in the regions that should be isothermal. In order to minimize this problem each wire is wrapped around its support several times before passing to another temperature region. This procedure insures that the anchor points of the wire are at the temperature of their support. All wiring is held in place by a coat of varnish.

The two ends of the sample wire are placed next to each other on the constant temperature rod. A twisted pair of copper leads is then connected to the sample with a solder joint and these leads are brought outside of the cryostat to be connected to a voltmeter. Since the two copper wires experience the same thermal environment, they should contribute no net voltage to that present across the sample. Consequently the voltage measured across the copper leads outside the cryostat will be essentially that generated by the sample.

As with the sample leads, all leads leaving the cryostat are twisted together in pairs to minimize electrical noise pick-up.

The length of the support rods is such that the sample passing between the two rods at the top is outside the solenoid. When it again crosses at the bottom it is in the central region of the solenoid. In order that this arrangement yield the desired information it is important that the sample be isothermal as it passes into the region of the solenoid. If it is not isothermal then unwanted thermoelectric voltages will be developed. In addition to the previously mentioned

precautions against this used for all wiring, one other thing is done. Heat conduction through the sample is minimized by making the length of the sample joining the two temperature regions as great as is practical. This was done by wrapping the sample several times around a thermally insulating synthane spool before attaching it thermally to the variable temperature rod.

The magnet used was an Oxford Instrument Company superconducting solenoid. A calibration table of magnet current vs. field strength was available, so the field strength did not have to be directly measured. To set the desired field all that had to be done was to adjust the solenoid current to the appropriate value. The current supply for the solenoid contains a circuit which automatically adjusts the current to any preset value within its operating range. The current was monitored by measuring the voltage drop across a .001 ohm resistor that was in series with the solenoid. Once the current had been set the solenoid was shorted out with a length of superconducting wire. The current then remained constant until the short was removed and the power supply reconnected.

One difficulty exists with this experimental arrangement. Though the top section of the sample is outside of the solenoid it still experiences the fringe field which exists around the magnet. According to Chiang the fringe field at the top position of the sample is about 1/100 of the central field. Since the largest field used is 50 kG the largest fringe field will be about .5 kG. To check on the importance of fringe field effects, measurements were made for small central fields. It was found that ΔS at .5 kG was negligibly small in comparison to ΔS for fields of 10 kG and higher.

All voltage measurements were made with digital voltmeters. The thermoelectric voltage from the sample was measured using a Keithley Model 180 digital nanovoltmeter with a resolution of ten nanovolts.

CHAPTER IV

SAMPLE PREPARATION

The samples were in the form of polycrystalline wires. They were prepared from Cominco 6N silver and Cominco 5N gold. The silver came in the form of small pellets. To remove surface contaminants, they were first etched in a 1:1 solution of ammonium-hydroxide: hydrogen-peroxide and then in nitric acid. The gold also came in the form of small pellets but was etched in aqua regia. As the first step in creating the required very dilute alloys a one atomic percent gold in silver alloy was made. This was diluted with appropriate amounts of silver to produce the desired concentrations. The gold and silver pellets were placed together in a graphite crucible and heated past their melting points to about 1400°K using an induction furnace. The resulting liquid was then agitated by rocking the crucible in order to create a homogeneous mix. The heated alloy was poured from the graphite crucible into a copper mold where it was allowed to cool. This was repeated a second time in order to further insure a homogeneous mixing of the gold and silver. After cooling, the rod was passed through a rolling mill to decrease its diameter and then through a series of successively smaller tungsten-oxide dies, and eventually diamond dies, until a wire with the diameter of .01" had been formed. The annealing of the samples will be discussed with the presentation of the data. The concentrations attempted were .1, .07, .04, and .03

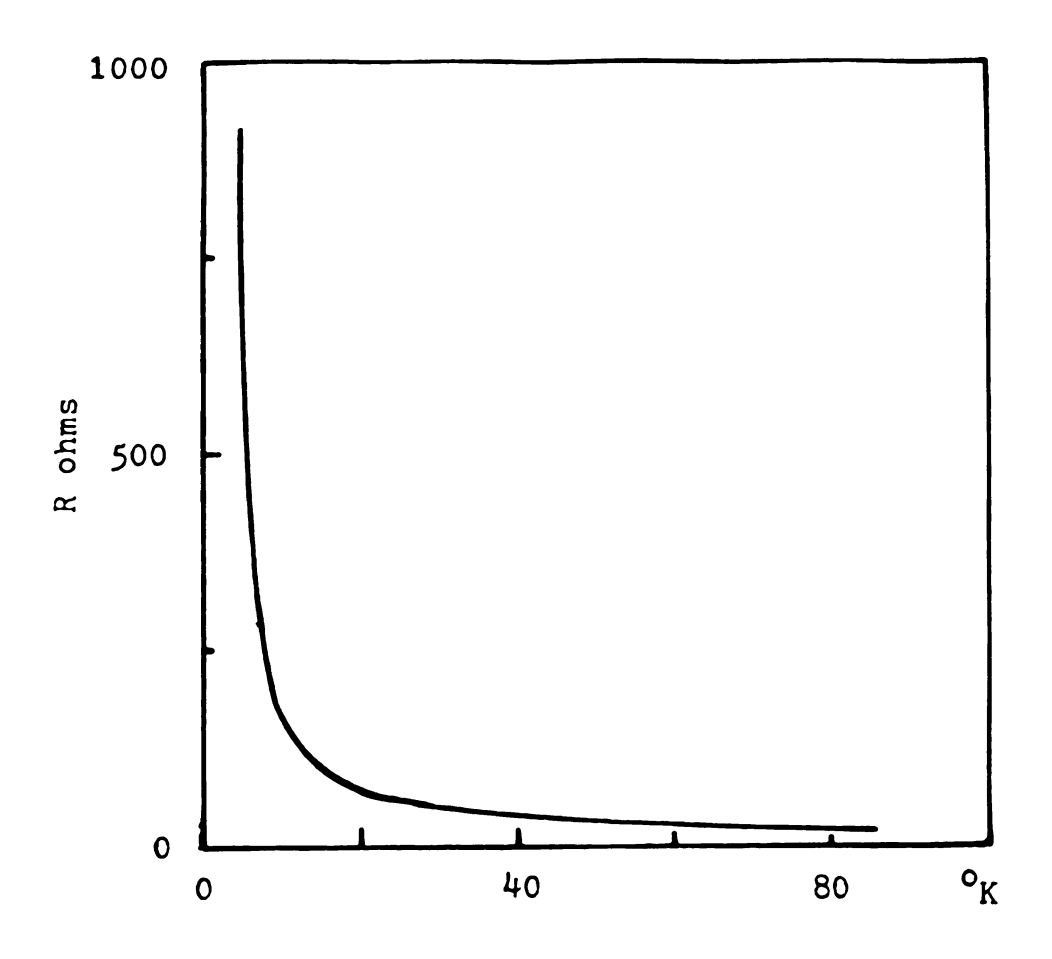
atomic percent gold in silver. When samples of these alloys were sent to Schwarzkopf Analytical they were reported as being .047, .048, .013, and .011 atomic percent gold in silver respectively.

CHAPTER V

DATA ANALYSIS

The data consist of thermometer resistances and sample EMFs. The first step in the data analysis is to convert the measured carbonglass resistances to their corresponding temperatures. A table of calibrated values from about 4°K to 85°K was available. It had been made by calibrating the carbon-glass resistor against a germanium resistance thermometer whose calibration was good to ± 1 percent. In order to estimate temperatures at points intermediate to the calibration points a curve was fitted to the R vs. T calibration points. From Figure 9 it is apparent that the LnR vs. LnT plot shows much less curvature than the direct R vs. T plot. A polynomial curve can be fitted to the ℓn plot much easier than the direct plot. The ℓnT , ℓnR calibration points were divided into four roughly equal temperature ranges and within each range the points were fit to a sixth degree polynomial using a computer program. Using these curves another computer program was used to generate a table of R vs. T in 5°mK increments from 4.190°K to 84.945°K. This table was then used to convert the carbon-glass resistance data to temperatures. The calibration data for the carbon-glass thermometer are included in an appendix along with the polynomial coefficients.

In order to calculate ΔS the EMF vs. T curve had to be differentiated. The EMF vs. T curve was found by breaking up the data into



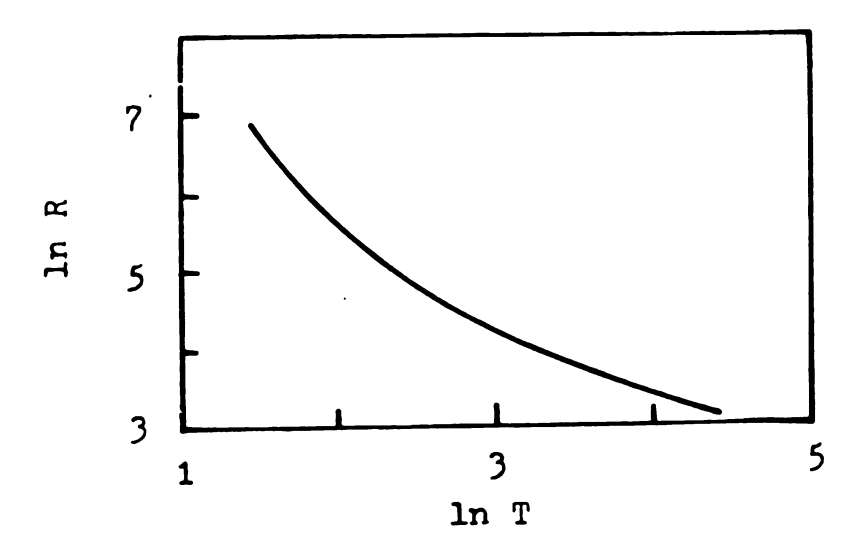
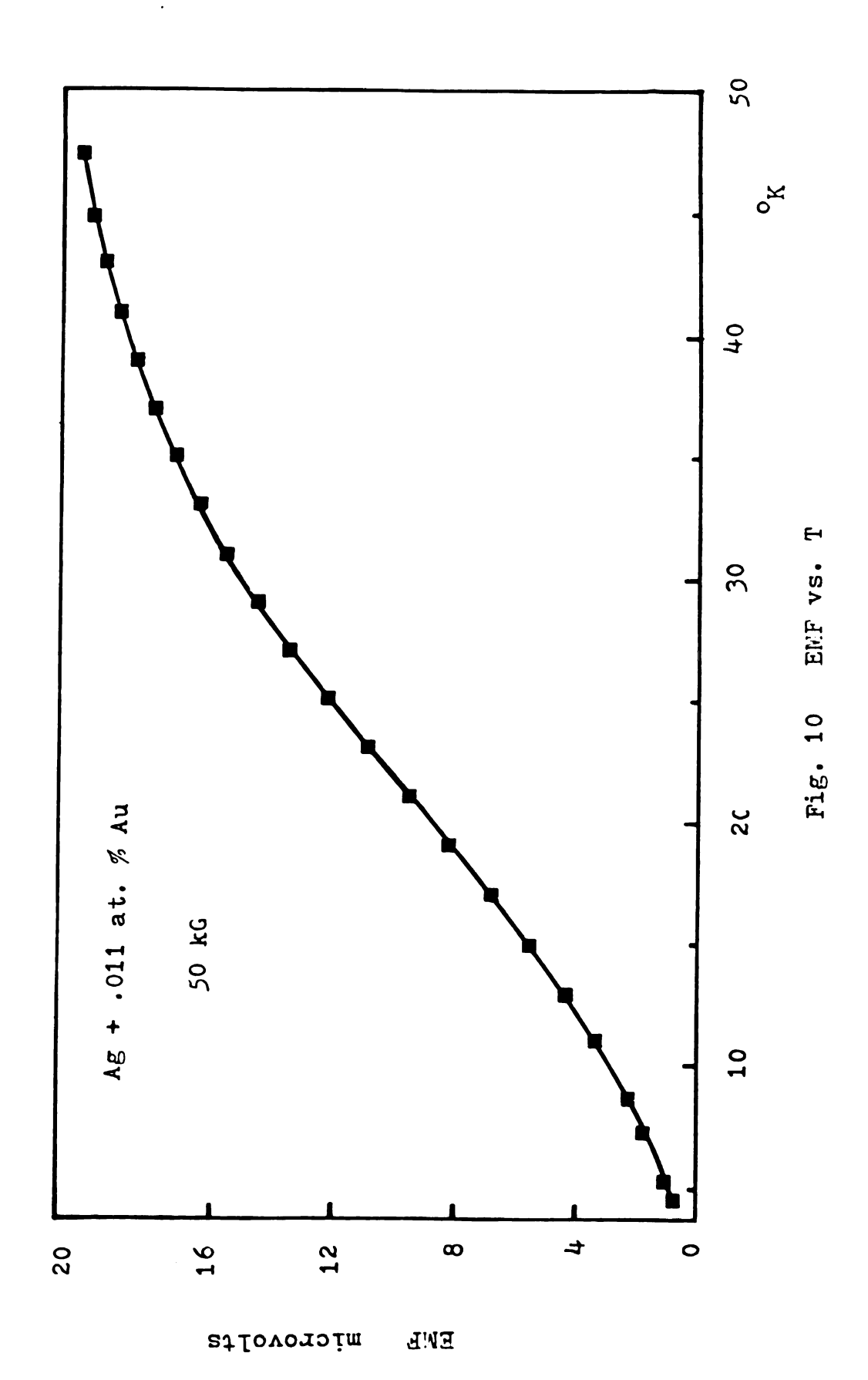


Fig. 9 Thermometer resistance

at most three temperature ranges and fitting the points within each range to a fourth-degree polynomial using a computer program.

Because of slight inhomogeneities in the sample wire and leads, the EMF is not strictly zero when no magnetic field is present. To account for this effect in the data, a zero field set of points for EMF vs. T was taken, and the resultant EMF vs. T curve was subtracted from the curve for non-zero fields. The output from the computer program consisted of calculated EMFs, S, and the coefficients of the polynomials used to fit the EMF vs. T data. The curve fitting was done by the least square method. Plots of some EMF data points along with their polynomial fit are shown in Figure 10.



CHAPTER VI

DISCUSSION OF RESULTS

One thing that became apparent was that the peak value of ΔS for the first samples done seemed much too small in comparison with the results of pure silver and silver +.37 at.% gold found by Chiang. The residual resistance ratios were measured and found to be inconsistent with those of Crisp and Rungis. This information is shown. in Table 1. It was thought that perhaps some unwanted impurity might have contaminated the alloys during the mixing process. The only things the alloys came in contact with while they were in the liquid state and most vulnerable to absorbing impurities were the copper mold and graphite crucible. The copper mold seemed the most likely candidate as a possible source of impurity. This was tested by measuring the resistance ratio of pure silver that had been melted in the graphite crucible and comparing it to the resistance ratio of a sample of pure silver that had been poured into the copper mold. The resistance ratios of both samples were essentially the same. With these results it seems unlikely that the copper mold was a source of impurities.

Another possibility was that something in the annealing procedure was responsible. It is known that very small amounts of iron can cause large effects in the thermopower of a material. One common way of removing these iron impurities is by annealing the alloys

Table 1. Data on Ag-Au Alloys

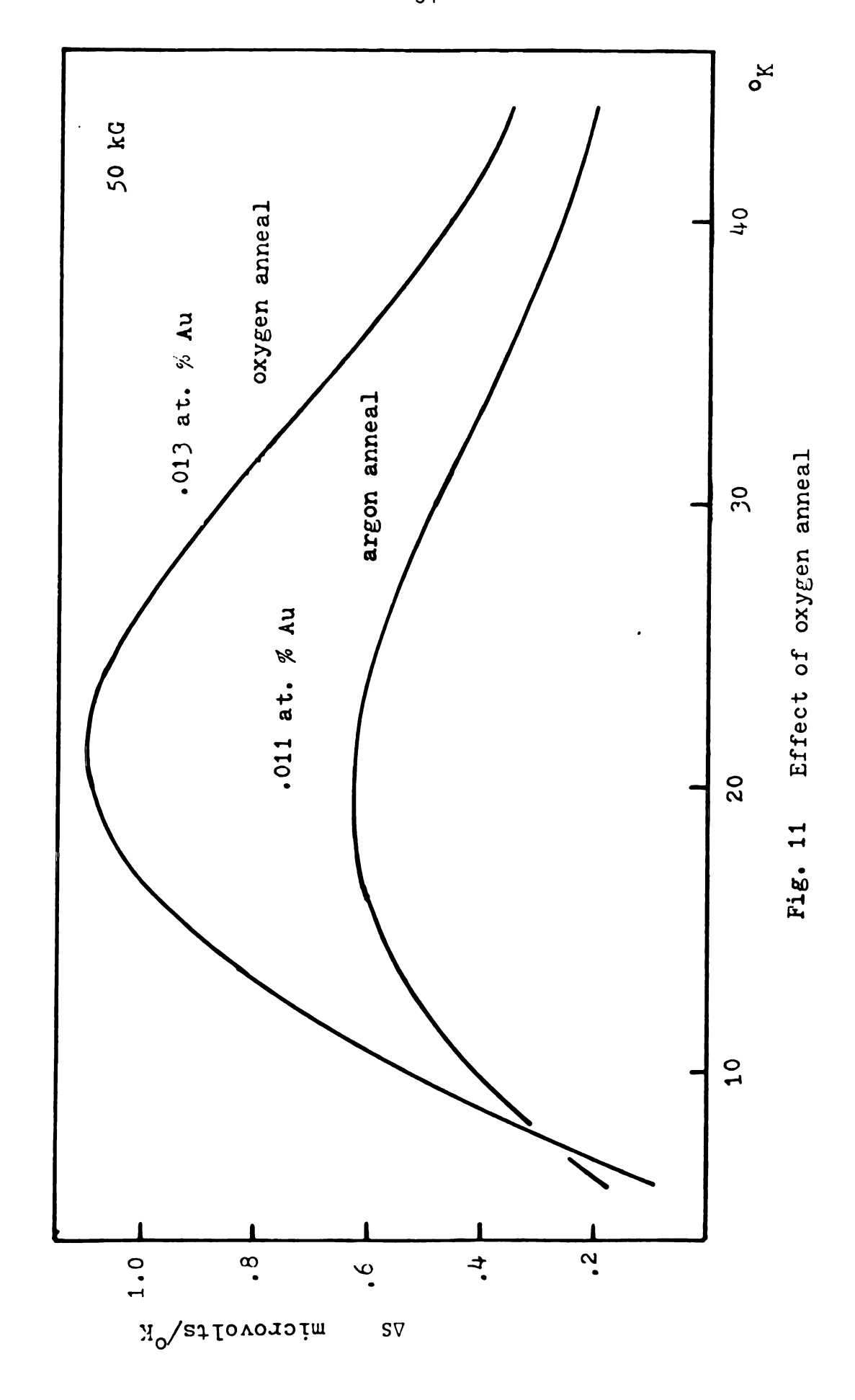
Atomic % Au	RRR	ΔS _{max} (μV/°K)	Annea1		
.011	49.4	. 625	argon		
.013	102	1.1	oxygen		
.047	45.6	.77	vacuum		
.048	50.7	.83	argon		
.000	540 (copper mold)		vacuum		
.000	542 (graphite mole	i)	vacuum		
.013	87.6		vacuum		
From Crisp and Rungis					
.000	700		oxygen		
.09	50		oxygen		
.69	7		oyxgen		
From C. K. Chiang					
.000	500	2.25	air		
. 37	11.5	.1	?		

RRR=Resistance Ratio= $\frac{R(273^{\circ}K)}{R(4.2^{\circ}K)}$

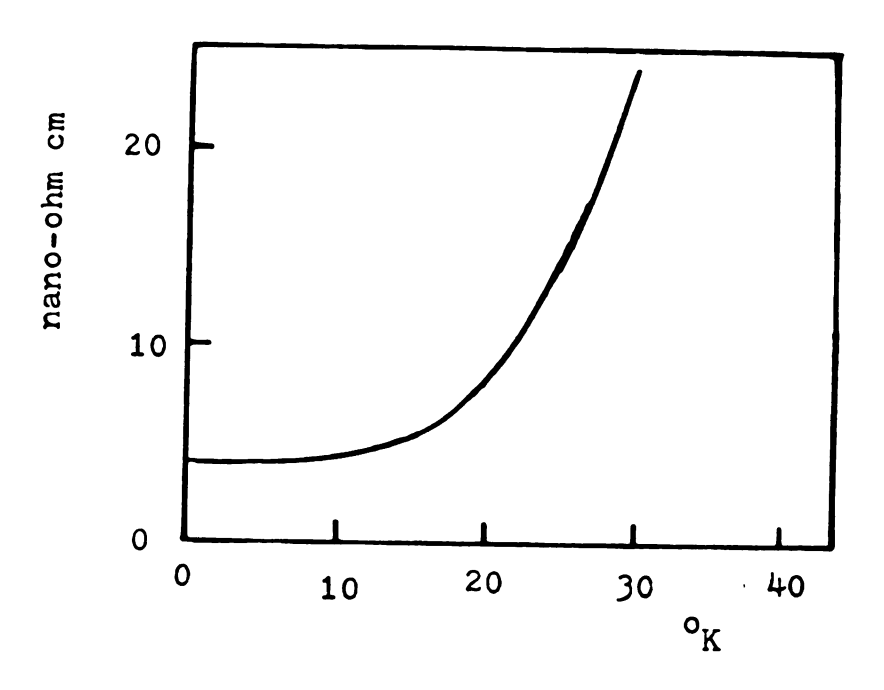
in oxygen. The previous samples had all been annealed in either vacuum or argon. To test this possibility a .013 at.% alloy was prepared; one sample of the alloy was annealed in vacuum and another in oxygen. The resistance ratio for the sample annealed in oxygen had the higher value. As can be seen from Figure 11 the peak value of ΔS for the .013 at.% sample annealed in oxygen was significantly greater than that of the .011 at.% sample which was annealed in vacuum. It seems likely then that small amounts of iron impurity were responsible for the small ΔS values.

It is common to try interpreting the behavior of ΔS in terms of $\omega \tau$. $\omega = \frac{eB}{mc}$ is the cyclotron frequency of a free electron and τ is the relaxation time from the simple conductivity relation $\sigma = ne^2 \tau/m$. Curves for materials other than those described in this thesis tend to show that the peak in ΔS moves to higher temperatures as the field strength is increased. Of the alloys studied in this thesis, only the .011 at.% alloy showed this trend. The trend is slight enough though that its validity may be questioned. If the peak were to occur at some particular value of $\omega \tau$, then it is evident from the graph of R vs. T in Figure 12 that the temperature at which the peak occurs would be expected to move much more than is observed.

Another effect which argues against the peak being simply related to $\omega\tau$ is the fact that as the concentration of gold in silver increases the peak in ΔS moves to a higher temperature. This is shown in Figure 13. If the $\omega\tau$ dependence were correct then the peak should move to lower temperatures where relaxation times have been shortened by the introduction of impurities.



Ag + .011 at. 70 Au



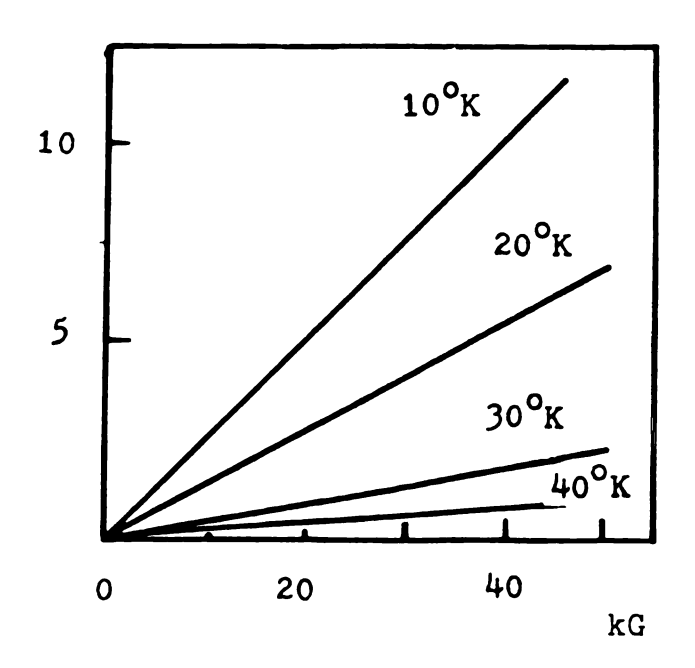


Fig. 12 Resistivity vs. T

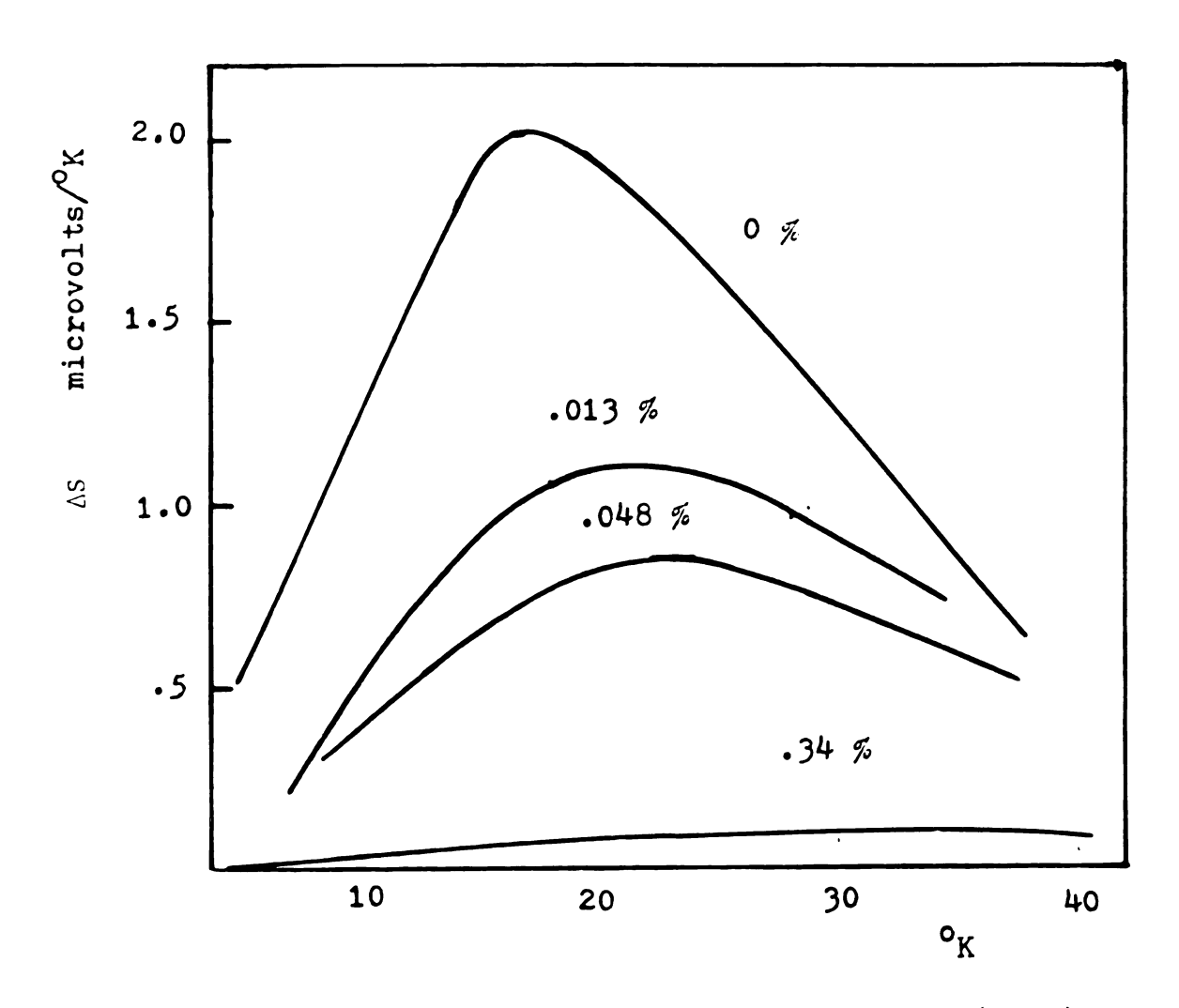


Fig. 13 Variation of ΔS with concentration (50 kG)

The one aspect in which the $\omega\tau$ viewpoint seems appropriate is in its implications for the ΔS vs. field strength characteristics of the samples for various temperatures. If the thermopower reaches a saturation value, it would seem reasonable for it to be related to $\omega \tau$ since this gives some indication of how noticeable the field is to the sample. For very short relaxation times an electron will barely begin to traverse its cyclotron orbit before it is scattered; the magnetic field is not likely to have a very great effect in this situation. At low temperatures only a small field is necessary in order to cause electrons to traverse their cyclotron orbits many times before being scattered. If ΔS has a saturation value it will likely reach it for fairly small fields at low temperatures. At higher temperatures correspondingly higher fields would be needed to push ΔS to its saturation value. The graphs in Figure 14 seem to suggest this sort of behavior. At the lower temperatures ΔS seems to be saturating. At the higher temperatures it also seems to be saturating but not to as great an extent.

The peak in ΔS and the phonon drag peak in S(H=0) (Figure 15) both occur in the same temperature region. This suggests that the ΔS peak may be associated with the phonon drag thermopower. As the concentration of gold is increased, the peak in S moves to lower temperatures while the peak in ΔS moves to higher temperatures. Because of this behavior it seems unlikely that ΔS is due simply to enhancement of the phonon drag peak.

As shown in Figure 13, the peak in ΔS is greatly reduced by the addition of small amounts of gold. Since the principal effect of the gold should be to scatter phonons, this evidence suggests that the peak in ΔS may be largely due to phonon drag thermopower.

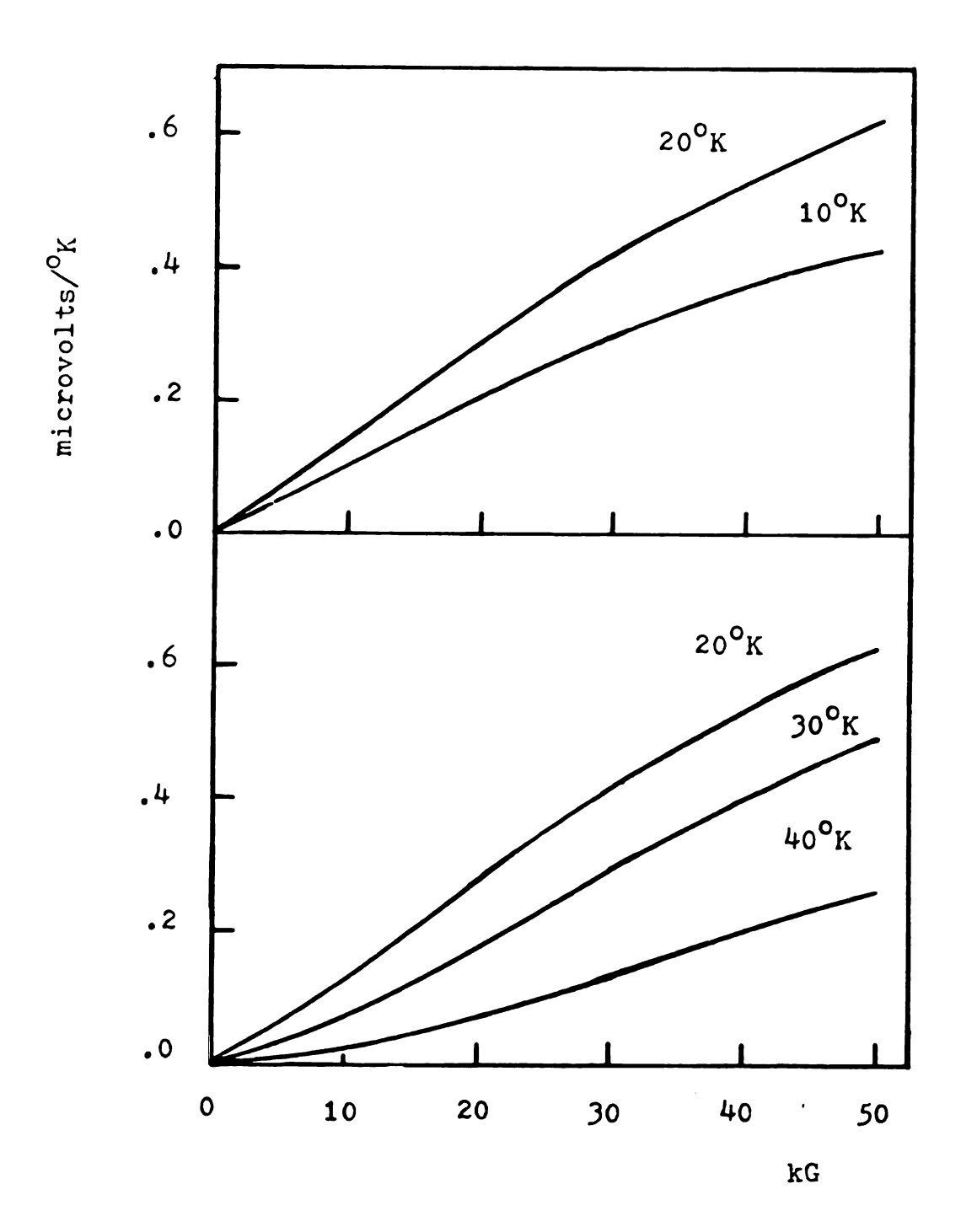


Fig. 14 \(\text{\subseteq}\) S vs. H

Ag + .011 at. % Au

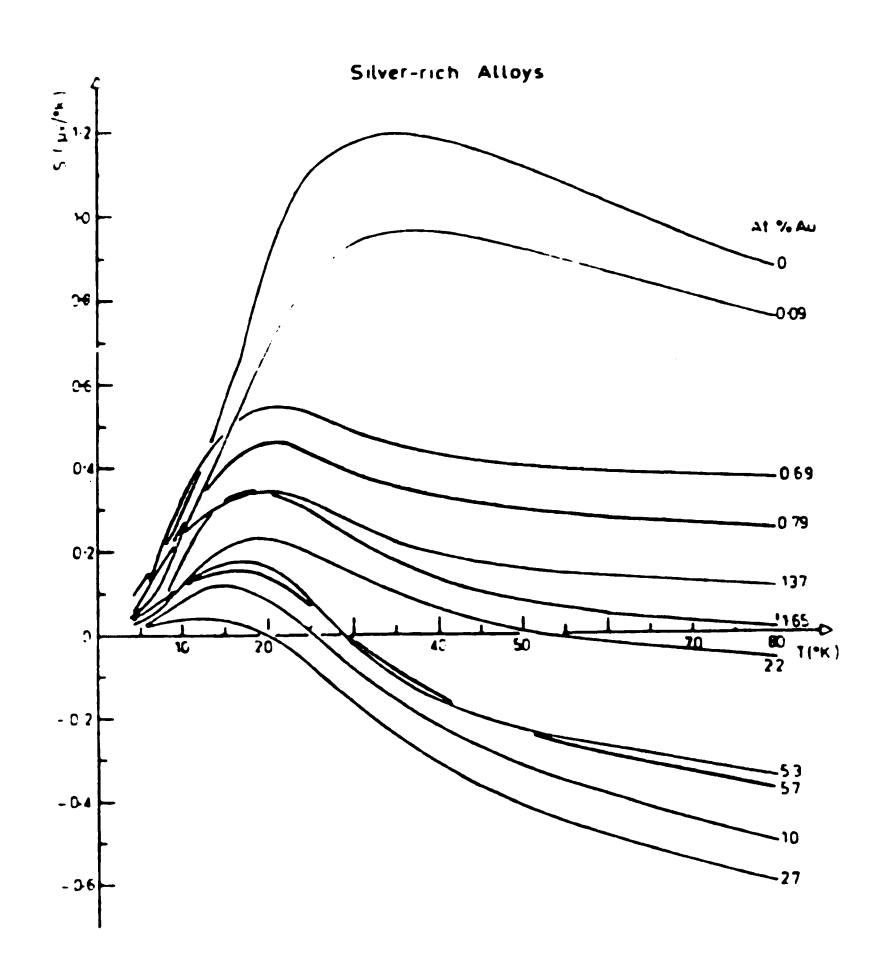


Fig. 15 Zero field thermopower ⁷

The relations $\Delta S = AT + BT^3$ and $\Delta S = AT + BT^{-1}$ can be used to see how much of the ΔS is due to phonon drag and how much to diffusion thermopower. By looking at graphs of $\Delta S/T$ at low temperatures and $T\Delta S$ at higher temperatures, the variation of the coefficients A and B may be seen. These graphs are shown in Figures 16 and 17. It is apparent from Figure 17 that A and B change proportionately, so if they truly represent diffusion thermopower and phonon drag thermopower then they are both affected equally by the magnetic field. ΔS is due equally to both diffusion theropower and phonon drag thermopower. In order to be more confident of this conclusion, the experimental curve should be extended well beyond where the phonon drag peak occurs, i.e. up to at least $100^{\circ}K$.

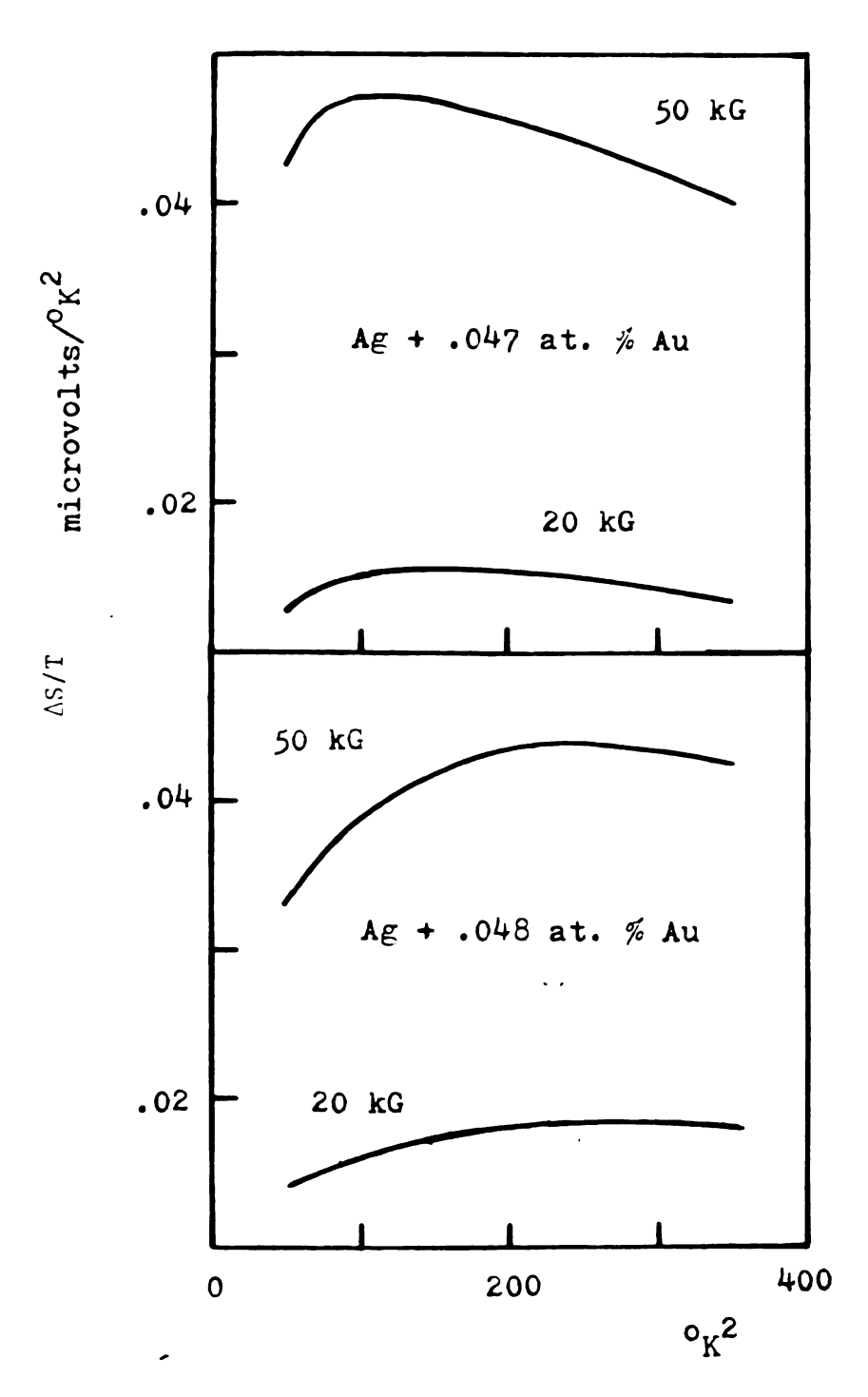


Fig. 16 Δ S/T vs. T^2

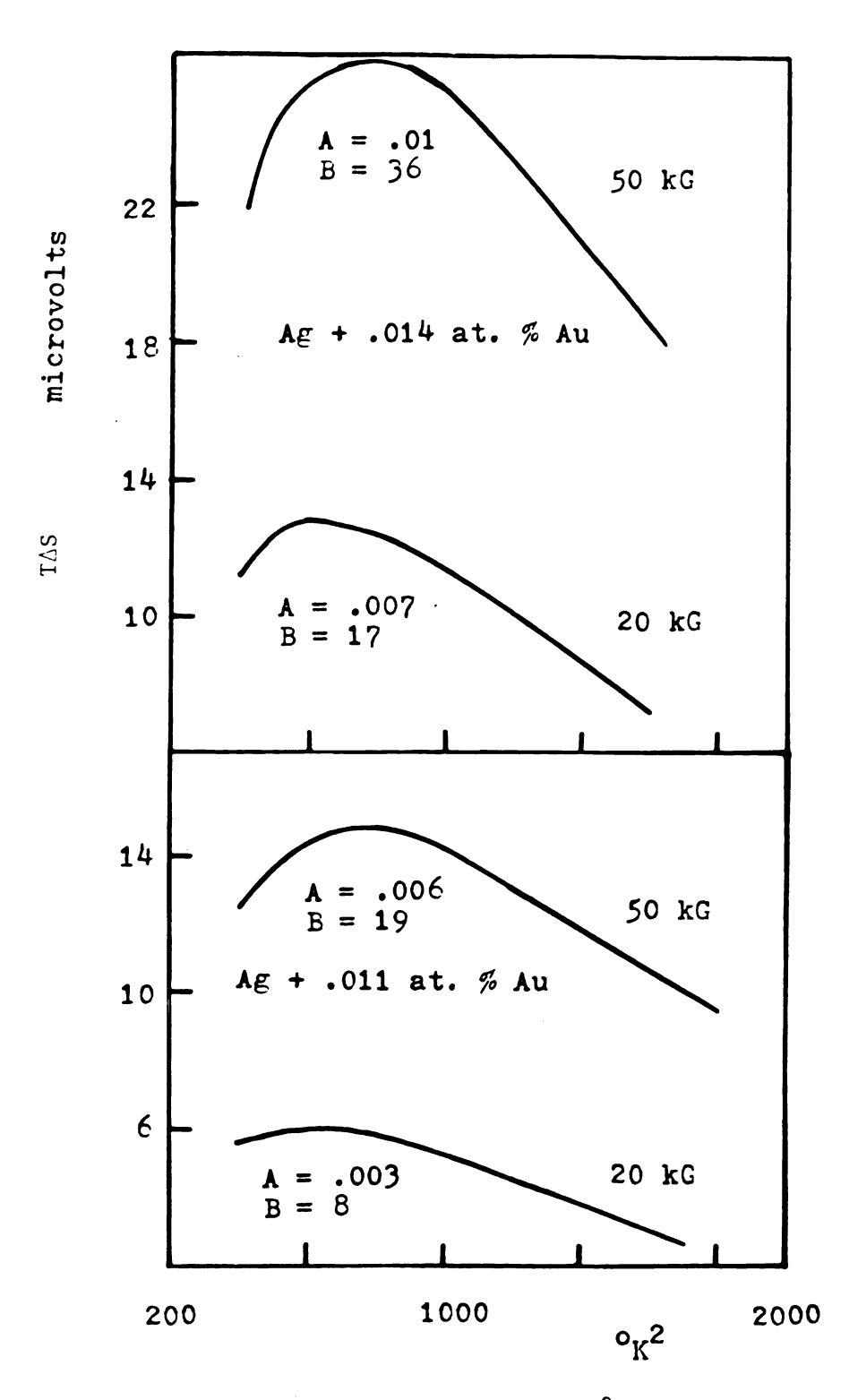
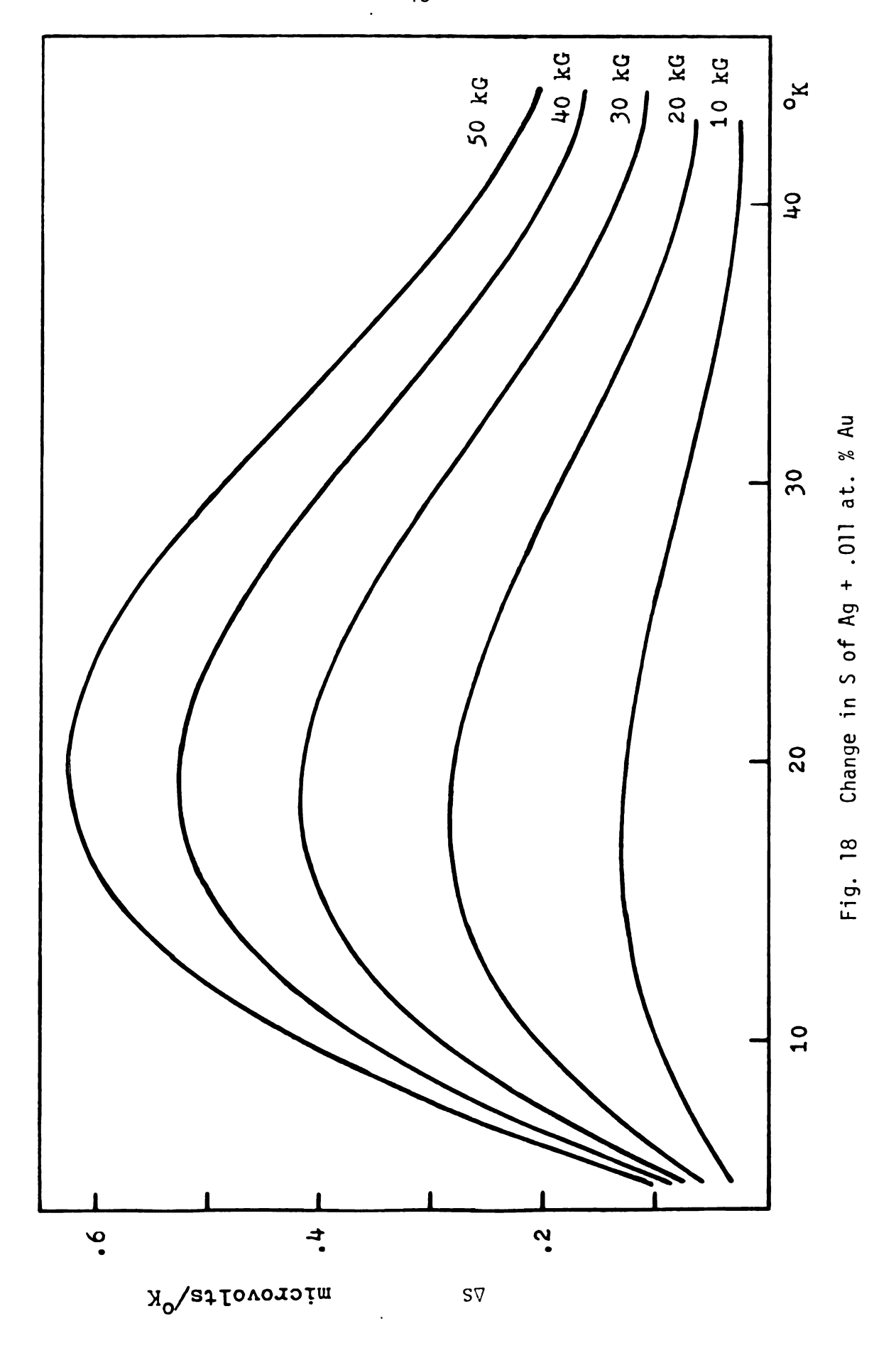
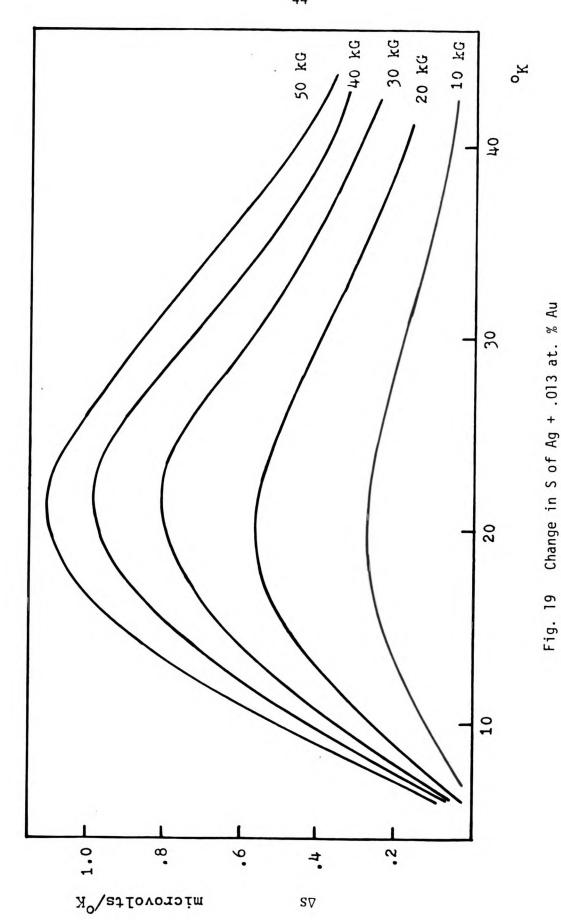
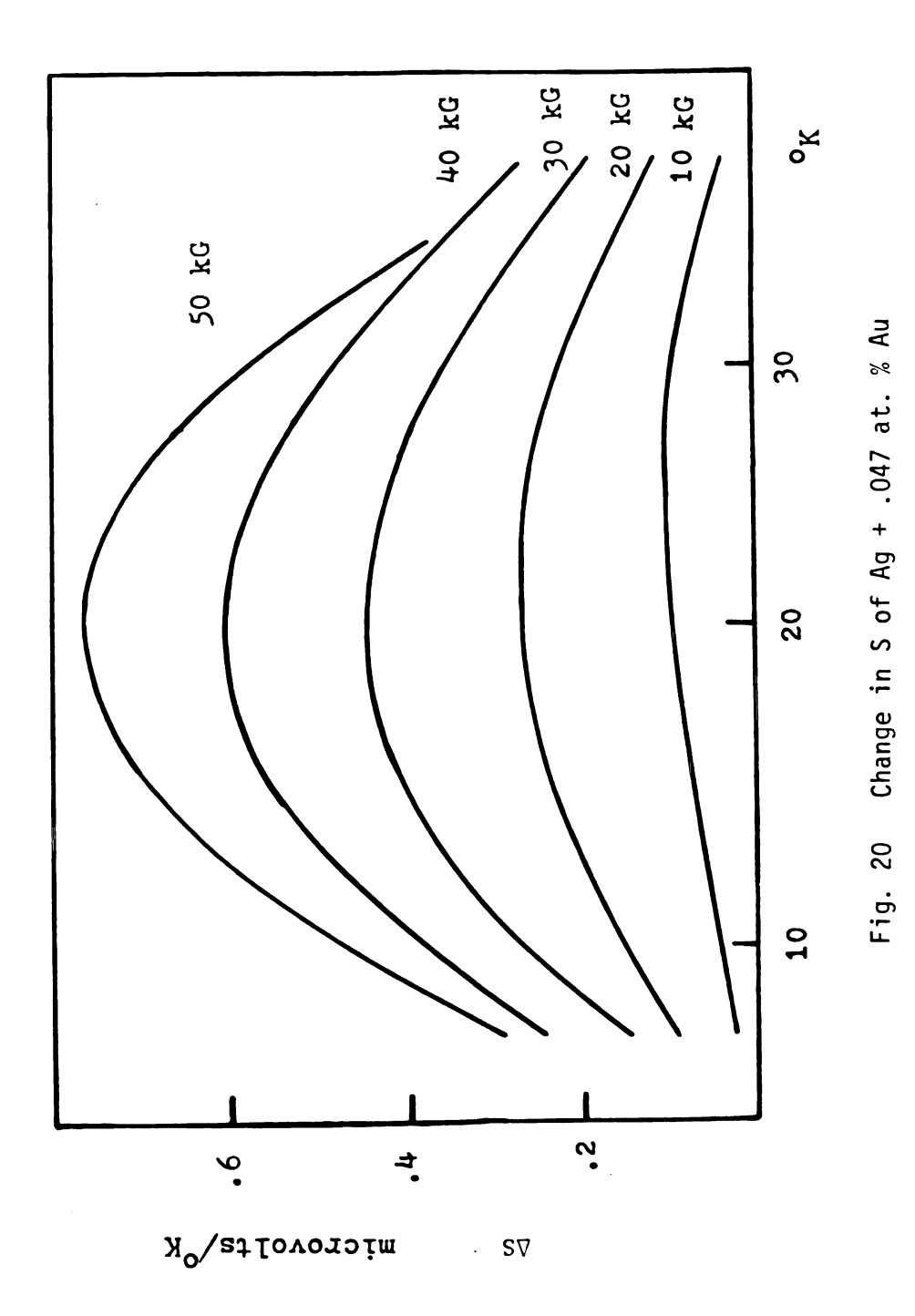
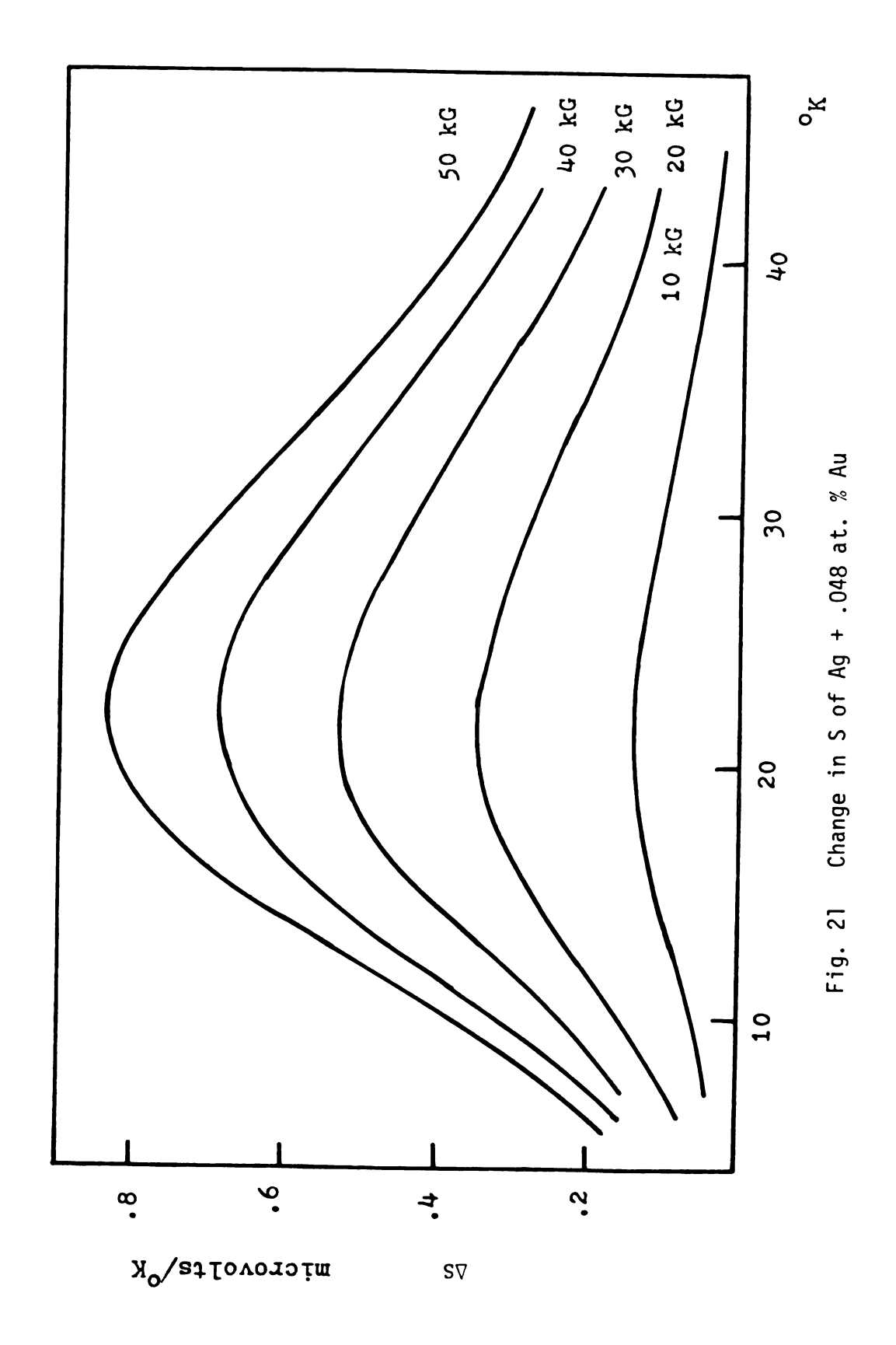


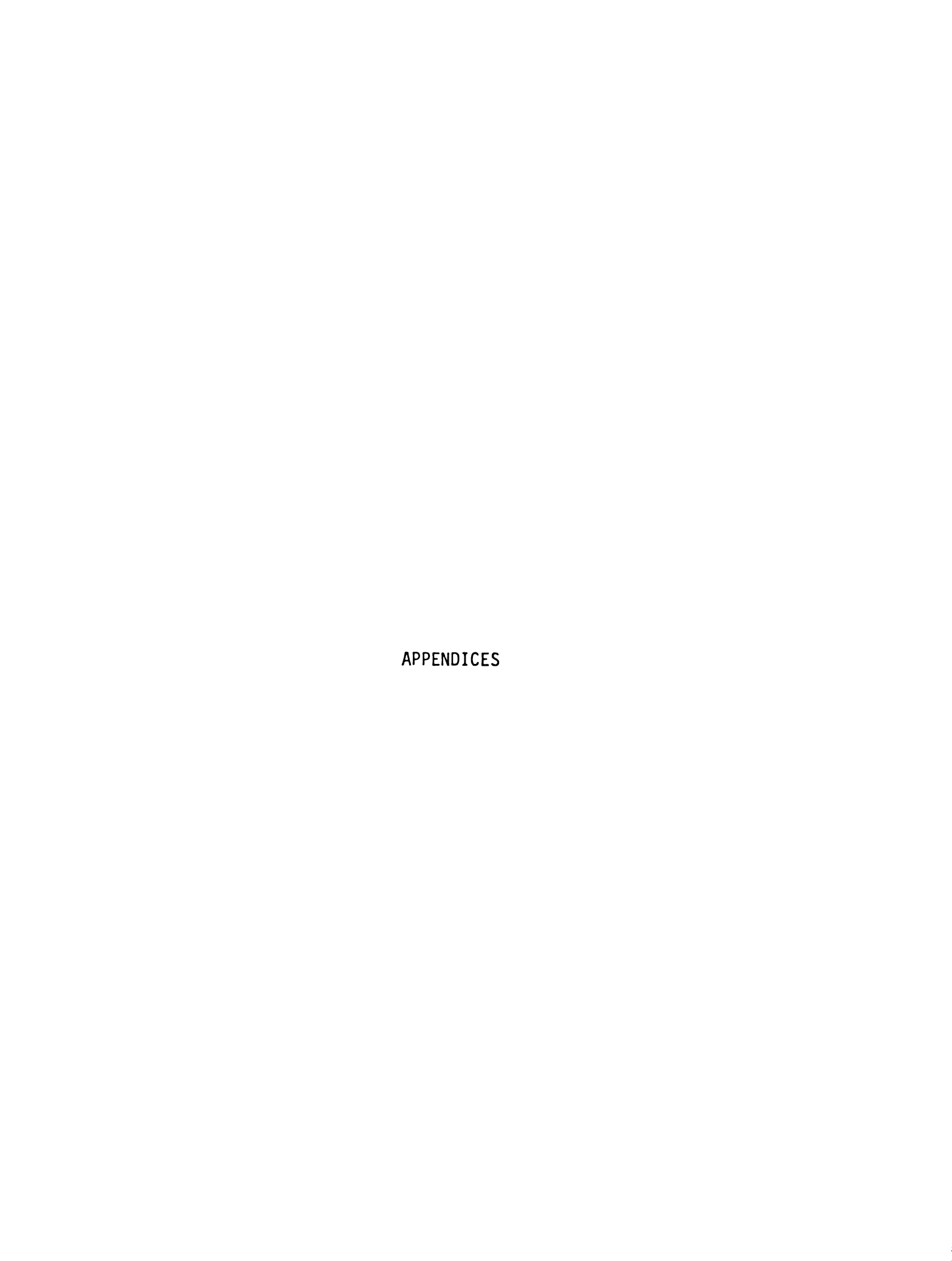
Fig. 17 T Δ S vs. T²











APPENDIX A

Table 2. Calibration Data for Resistance Thermometer*

Temperature °K	Resistance Ω	Temperature °K	Resistance Ω
4.191	937.2	14.355	95.80
4.192	936.4	15.319	88.755
4.307	894.1	15.810	85.26
4.309	893.8	17.057	78.57
4.322	888.2	18.202	73.305
4.378	862.65	18. 6 18	71.375
4.383	861.9	19.410	68.43
4.557	783.7	19.890	66.7 8
4.738	701.4	20.630	64.405
4.863	666.8	21.223	62.66
5.183	560.1	21.710	61.315
5.779	437.25	22.600	58.965
6.098	388.8	24.913	54.065
6.230	371.8	27.093	50.325
6.405	351.1	29.641	46.78
6.800	310.3	31.292	44.845
7.089	286.0	33.224	42.85
7.266	273.05	34.364	41.79
7.563	253.8	36.083	40.32
7.942	231.5	37.799	39.05
8.310	213.75	40.648	37.14
8.743	196.05	43.607	35.43
9.249	178.7	48.326	33.225
10.068	155.95	52.390	31.635
10.731	141.95	57.097	30.06
11.404	129.9	62.460	28.6095
11.755	124.6	70.022	26.9275
12.202	118.35	77.425	25.5918
12.922	109.75	77.927	24.532
13.267	105.95	84.949	24.4695
13.760	101.1		

^{*}Carbon Glass Resistor #842, Lake Shore Cryotronics, Inc.

Table 3. Coefficients used for Polynomial fit to Resistance Data

$$\ln R = A + B \ln T + C(\ln T)^2 + D(\ln T)^3 + E(\ln T)^4 + F(\ln T)^5$$

4.191°K to 5.183°K

A = -.1889066E+04 B = .4921020E+04 C = -.4783237E+04 D = .2064272E+04 E = -.3339054E+03 E = .0000000E+00

4.863°K to 8.310°K

A = .6727089E+02 B = -.1216509E+03 C = .9345597E+02 D = -.3258694E+02 E = .4280011E+01 F = .0000000E+00

7.942°K to 21.223°K

A = .1424817E+02 B = -.8333470E+01 C = .2962758E+01 D = -.5773279E+00 E = .4773964E-01 F = .0000000E+00

20.630°K to 84.949°K

A = .1377278E+02 B = -.7123667E+01 C = .2040751E+01 D = -.2946827E+00 E = .1702847E-01 F = .0000000E+00

APPENDIX B

COMPUTER PROGRAM USED TO FIT EMF DATA TO A POLYNOMIAL

```
CC... DATA BECK MUST END WITH TWO TRIPLE ZERO CARDS ...

C CALL INPUT (HEADING ON PTS OF TO FMF)

IF (NPTS OLT OLD ON PTS OT OTHER)

CALL FIT (NPTS OT OTHER ON PTS OT OTHER)

CALL INPUT (HEADING ON PTS OTO THER)

CALL OUTPUT (HEADING ON PTS OTO THERE OTHERS OTHERS)

CALL OUTPUT (HEADING ON PTS OTO THE OTHER OTHERS OTHERS
```

```
CONDENS ON THE FIRST DATA GROUP IS SUBTRACTED FROM THE FIT TO EACH OF THE SUCCEDING DATA GROUPS.

HAT PAIR PRINCE PRINCE DATA POINTS

CONDECTED TO THE FIRST DATA GROUP IS SUBTRACTED FROM THE FIT TO EACH OF THE SUCCEDING DATA GROUPS.

FEAD 900.(HEADING(I).I=1.8)

OCCUPANTION OF THE FIRST DATA GROUP IS SUBTRACTED FROM THE FIT TO EACH OF THE SUCCEDING DATA GROUPS.

FEAD 900.(HEADING(I).I=1.8)

OCCUPANTION OF THE FIRST DATA GROUP IS SUBTRACTED FROM THE FIT TO EACH OF THE SUCCEDING DATA GROUPS.

FEAD 900.(HEADING(I).I=1.8)

OCCUPANTION OF THE FIRST DATA GROUP IS SUBTRACTED FROM THE FIT TO EACH OF THE SUCCEDING DATA GROUPS.
```

```
SUPROUTING FIT(NPTS-T-FMF-COFF)
PIMERSION T(100)-EMM (100)-COFF(5)-COL1(5)-COL2(5)-COL3(5)-COL4(5)
CIMERSION COL5(5)-COLZ(5)
0000
          THIS SUBROUTING DOES A LEAST SQUARES FIT TO THE T-EMF DATA TO FIND EMF AT A FOURTH DEGREE POLYNOMIAL IN T.
             PO 10 I=1.5

(OL1(T)=0.0

00 20 J=1.NPTS

COL1(I)=COL1(I)+T(J)++(I-1)
       20 CONTINUE
r
       00 39 T=1+5

(0L2(1)=0+0

00 40 J=1+NPTS

(0L2(1)=COL2(1)+T(J)++1

45 (ONTINUE

35 CONTINUE
C
              00 50 [=1.5
C0L3(I)=0.0
D0 60 J=1.NPTS
C0L3(I)=C0L3(I)+T(J)++(I+1)
C0NJINUF
       60 CONTINUE
C
      | NO 79 | 1=1.5
| COL4(1)=0.0
| DO 80 J=1.NPTS
| COL4(I)=COL4(I)+T(J)++(I+2)
| RO | CONTINUE
| 70 | CONTINUE
C
       DO 90 I=1.5

COL5(1)=0.0

DO 100 J=1.0PTS

COL5(1)=COL5(1)+T(J)++(1+3)

OO CONTINUE

90 CONTINUE
    CALL DIPMNT(COL1.COL2.COL3.COL4.COL5.DFT)
CALL DIPMNT(COL2.COL2.COL3.COL4.COL5.DFT1)
CALL DIPMNT(COL1.COL2.COL3.COL4.COL5.DET2)
CALL DIPMNT(COL1.COL2.COL3.COL4.COL5.DET2)
CALL DIPMNT(COL1.COL2.COL3.COL4.COL5.DET4)
CALL DIPMNT(COL1.COL2.COL3.COL4.COL7.DET5)
Ç
              COEF(1) = DE T1/DET
COFF(2) = DE T2/DET
COEF(7) = DE T3/DET
COEF(4) = DE T4/DET
COEF(5) = DE T5/DET
r
              RETURN
ND
```

```
SUPPOUTITY OUTPUTCH: ADIMC+MPTS+T+FMF+COFF+HASE)
TIMESION T(100)+FMF(100)+CMFF(5)+MASE(5)
JUTLGER OHNADING(*)
         T-TUMP=TEMFFRATURE (DIGREES KELVIR)
EME=MFASUPID VOLTAGE (MICROVOLIS)
CUMF-CALCULATED EME COPPECTED FOR ZEPO FIELD EME
DUTATESCALCULATED EME COPPECTED FOR ZEPO FIELD EME
DUTATES-CHANGS OF TEP DUE TO MAGDETIC FIELD (MICROVOLIS PUR DEGREE KELVIN)
      IRINI 1000 (HEADING(1) + I=1 + R)

PRINT 9 0

CHICS=0 0

D) 20 J=1 + 5

CCME=CEME + COEFC(J) + T(I) + + (J-1)

20 CHICS=0 0

D) 20 J=1 + 5

CCHME = CEME + COEFC(J) + T(I) + + (J-1)

CCHME = CEME + COEFC(J) + T(I) + + (J-1)

CCHME = CEME + (COEFC(J) + RASI(J) + T(I) + + (J-1)

CCHME = CCEME + (COEFC(J) + RASI(J) + T(I) + + (J-1)

CCHME = CCEME + (COEFC(J) + RASI(J) + T(I) + + (J-1)

CONTINUE

DLIATIP= DLIATEP + (J-1) + (COEFC(J) + RASE(J) + T(I) + + (J-2)

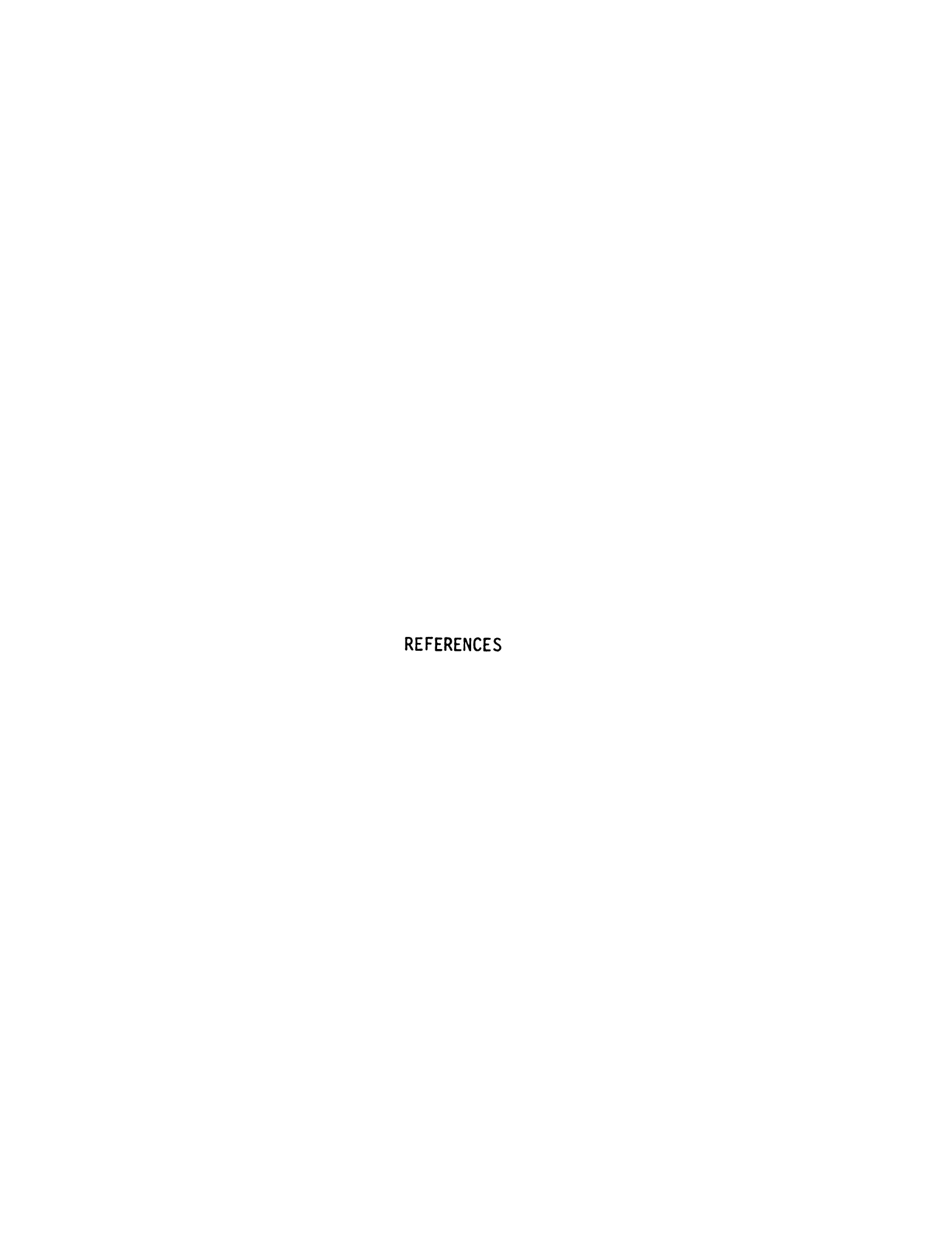
TONTINUE

PRINT 910 + T(I) + EME(I) + CCEME + DLIATEP

10 (ONTINUE

AVESTRESCRI(CHISQ/*PTS)

POLITIC 911 + AVESTRESCRI
               AVESURTESQRT (CHISQZMPTS)
PRINT 911.AVESURT
PRINT 912.COEF(J).J=1.5)
C
               PRINT 919
TEHP=4.0
C
              5 .
       .; ი
    PLIURM
                . 46
```



REFERENCES

- A. D. Caplin, C. K. Chiang, J. Tracy, P. A. Schroeder, Phys. Stat. Sol. (a) <u>26</u>, 497 (1974).
- 2. F. J. Blatt, C. K. Chiang, L. Smrcka, Phys. Stat. Sol. (a) <u>24</u>, 621 (1974).
- 3. F. Napoli, D. Sherrington, J. Phys. F, L53 (1971).
- 4. R. D. Barnard, "Thermoelectricity in Metals and Alloys", Taylor & Francis, Ltd., London (1972).
- 5. F. J. Koch and R. F. Doezema, Phys. Rev. Lett., 24, 507 (1970).
- 6. C. K. Chiang, Rev. Sci. Inst. 45, 37 (1974).
- 7. R. S. Crisp and J. Rungis, Philos. Mag. 22, 217 (1970).
- 8. C. K. Chiang, unpublished.
- 9. F. J. Blatt, P. A. Schroeder, C. L. Foiles, D. Greig, "Thermoelectric Power of Metals", Plenum Press, New York (1976).

